

Unlocking Multimodal Mathematical Reasoning via Process Reward Model

Ruilin Luo^{12*} Zhuofan Zheng^{2*} Yifan Wang¹ Xinzhe Ni¹
 Zicheng Lin¹ Songtao Jiang³ Yiyao Yu¹ Chufan Shi¹
 Lei Wang⁴ Ruihang Chu^{1†} Jin Zeng^{2†} Yujiu Yang¹

¹Tsinghua University ²ByteDance
³Zhejiang University ⁴ Ping An Technology (Shenzhen) Co., Ltd.

Abstract

Process Reward Models (PRMs) have shown promise in enhancing the mathematical reasoning capabilities of Large Language Models (LLMs) through Test-Time Scaling (TTS). However, their integration into multimodal reasoning remains largely unexplored. In this work, we take the first step toward unlocking the potential of PRMs in multimodal mathematical reasoning. We identify three key challenges: (i) the scarcity of high-quality reasoning data constrains the capabilities of foundation Multimodal Large Language Models (MLLMs), which imposes further limitations on the upper bounds of TTS and reinforcement learning (RL); (ii) a lack of automated methods for process labeling within multimodal contexts persists; (iii) the employment of process rewards in unimodal RL faces issues like reward hacking, which may extend to multimodal scenarios. To address these issues, we introduce **URSA**, a three-stage **U**nfolded **R**emaining **S**tructure **A**ided training framework. We first construct **M**ath**C**o**T**-1M, a high-quality large-scale multimodal Chain-of-Thought (CoT) reasoning dataset, to build a *stronger math reasoning foundation MLLM*, URSA-8B. Subsequently, we go through an automatic process to synthesize process supervision data, which emphasizes both logical correctness and perceptual consistency. We introduce DualMath-1.1M to facilitate the training of URSA-8B-RM. Finally, we propose **P**rocess-**S**upervised **G**roup-**R**elative-**P**olicy-**O**ptimization (**PS-GRPO**), pioneering a *multimodal PRM-aided online RL method* that outperforms vanilla GRPO. With PS-GRPO application, URSA-8B-PS-GRPO outperforms Gemma3-12B and GPT-4o by 8.4% and 2.7% on average across 6 benchmarks. Code, data and checkpoint can be found at <https://github.com/URSA-MATH>.

1 Introduction

Following the substantial progress of Large Language Models (LLMs) in math reasoning [1–8], the math reasoning capabilities of Multimodal Large Language Models (MLLMs) have increasingly garnered attention [9–13]. Previous work has typically focused on aspects such as math reasoning data curation [14–18], training math-intensive vision encoders [19, 20], enhancing vision-language alignment [11, 21], or the application of post-training techniques [22–24, 13]. Given the success of Process Reward Models (PRMs) in improving LLM reasoning through methods like Test-Time Scaling (TTS) [25, 26] and Reinforcement Fine-Tuning (ReFT) [27, 28], the application of PRMs to multimodal reasoning remains unexplored.

* Equal contribution. Work done during Ruilin’s internship at ByteDance. † Corresponding author.
 ruihangchu@gmail.com, zengjin@bytedance.com

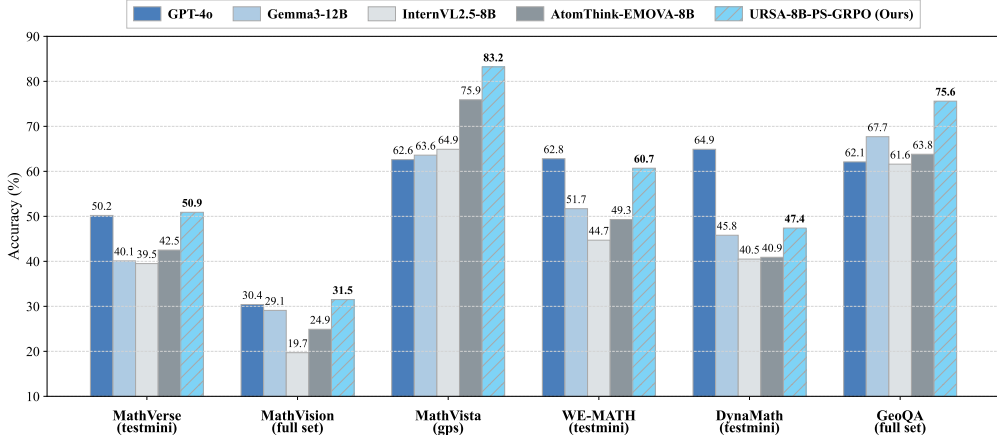


Figure 1: Performance comparison with leading open-source MLLMs and GPT-4o.

In this work, we take the first step toward integrating PRMs into multimodal math reasoning. We identify three key challenges: (i) Since both TTS and RL are heavily influenced by the strength of foundation models [29, 25], the limited availability of large-scale, high-quality reasoning data constrains the upper bounds of current MLLMs and weakens the effectiveness of PRM integration; (ii) There hasn't yet been adequate automated process labeling techniques merged within multimodal contexts, where both logical validity and perceptual consistency should be emphasized [30–32]. (iii) While PRMs can be effectively used in TTS, applying them directly in online RL introduces risks such as reward hacking and length bias in rewarding [33, 34].

To address these challenges, we propose the **URSA** framework, a three-stage Unfolding multimodal pRocess-Supervision Aided training pipeline that supports both the construction and application of multimodal PRMs. In Stage I, we curate **MMathCoT-1M**, a large-scale, high-quality multimodal Chain-of-Thought dataset synthesized from 1.43 million open-source examples, which enhances the foundation model's reasoning capabilities through targeted instruction tuning. In Stage II, we construct **DualMath-1.1M** via a dual-view process supervised data synthesis strategy which combines a binary error locating engine and a misinterpretation insertion engine. It provides complementary signals for logical validity and visual grounding, and is used to train a process reward model. In Stage III, we analyze the limitations of scalar process reward modeling in online RL and propose **Process Supervision-GRPO (PS-GRPO)**, which mitigates reward hacking and PRM's length bias in rewarding by implicitly penalizing process-level inconsistencies during policy optimization.

Results on 6 multimodal reasoning benchmarks show that our PRM improves Best-of-N verification, surpassing self-consistency and outcome-based baselines. When used in PS-GRPO, the resulting model achieves state-of-the-art performance among open-source MLLMs of similar size. Our contributions are as follows:

- We release two large-scale open-source datasets, MMathCoT-1M and DualMath-1.1M, to address the scarcity of high-quality multimodal CoT reasoning and process supervision data.
- We propose PS-GRPO, an online reinforcement learning algorithm that incorporates multimodal PRMs by comparing the relative quality of rollouts, rather than relying on scalar reward modeling. It effectively mitigates PRM's reward hacking and length bias in rewarding.
- Experimental results show that our reward model improves both test-time verification and online training. With PS-GRPO application (Figure 1), URSA-8B-PS-GRPO outperforms Gemma3-12B and GPT-4o by 8.4% and 2.7% on average across 6 benchmarks.

2 Stage I: Math-Intensive Alignment and Instruction Tuning

2.1 Collection of Vision-Language Alignment Data

We employ a LLaVA-like architecture and first collect vision-language alignment data directly from existing open-source datasets [35–38]. As demonstrated in Figure 2, we collect URSA-Alignment-860K from Multimath [23], MAVIS [19] and Geo170K [18]. We then filter out samples with overly

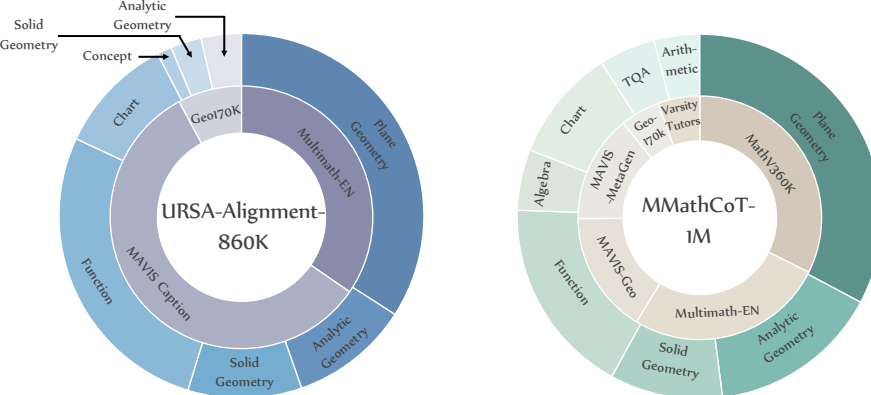


Figure 2: Statistics of URSA-Alignment-860K and MMathCoT-1M.

verbose captions, to form an 860K math-intensive alignment dataset. Following the engineering practices of previous work, we only train the MLP projector in the alignment step.

2.2 CoT Reasoning Data Synthesis

For a powerful foundation building, we collect 1.43M samples from existing math reasoning datasets to support the construction of large-scale CoT reasoning data. As shown in Figure 2, data is sourced from MathV360K [15], Multimath [23], MAVIS [19], Geo170K [18] and VarsityTutors [11]. Based on the type of solution, we categorize the data into *answer-only*, *analysis-formatted*, and *CoT-formatted*. We adopt different synthesis strategies for them to curate high-quality CoT reasoning trajectories. We utilize Gemini-1.5-Flash-002 (refer to \mathcal{G} below) as a cost-effective tool for data curation, avoiding expensive large-scale manual annotation.

CoT Expansion. For *answer-only* data $\mathcal{D}_1 = \{(x_i, y_i)\}_{i=1}^{N_1}$, such as MathV360K [15], each sample contains a question x_i and a ground-truth answer y_i . This type of data is heavily used in previous works for fast thinking reasoning mode [15, 11, 16]. However, answer-only training restricts the model from fully capturing the problem-solving process. It may lead to memory-based reasoning, hindering the model’s ability to directly provide answers to more complex reasoning problems [39]. We expand certain scale CoT reasoning trajectories for this category of data. Given a expansion prompt \mathcal{P}_C , we provide x_i and y_i , then prompt \mathcal{G} to output the reasoning trajectory leading to the answer y_i , yielding the expanded solutions $\mathcal{S}_{Ao} = \mathcal{G}(\mathcal{P}_C; \{x_i, y_i\}_{i=1}^{N_1})$.

Rewriting. This strategy is designed for *analysis-formatted* samples, denoted as $\mathcal{D}_2 = \{(x_i, y_i, a_i)\}_{i=1}^{N_2}$. This includes datasets like MAVIS-Geo, MAVIS-MetaGen [19], VarsityTutors [11], and Geo170K-QA [40]. Each sample contains a question x_i , an answer y_i , and textual analysis a_i . While this type of data provides walkthroughs, it often suffers from two issues: (i) It lacks strict step-by-step logic, exhibiting jumps in language or reasoning. (ii) A significant portion of the answers are relatively brief and cannot provide rich rationale. Given a rewriting prompt \mathcal{P}_R , we utilize \mathcal{G} to transcribe these solutions, thereby enhancing their step-by-step reasoning trajectories and linguistic diversity, resulting in the rewritten set $\mathcal{S}_{An} = \mathcal{G}(\mathcal{P}_R; \{x_i, y_i, a_i\}_{i=1}^{N_2})$.

Format Unification. This strategy is used for *CoT-formatted* data, primarily sourced from Multimath-EN-300K [23], which is collected from K-12 textbooks and contains mathematical language and symbolic-style reasoning solutions. This portion of the data, $\mathcal{D}_3 = \{(x_i, y_i, c_i)\}_{i=1}^{N_3}$, consists of a question x_i , an answer y_i , and a solution c_i . We unify the format through natural language stylization using a prompt \mathcal{P}_F with \mathcal{G} , producing the unified set $\mathcal{S}_C = \mathcal{G}(\mathcal{P}_F; \{x_i, y_i, c_i\}_{i=1}^{N_3})$.

MMathCoT-1M. Finally, we filter out instances where: (i) Correctness is violated: the generated content altered the original answer, or (ii) Consistency is problematic: the solution includes text that questions the original answer or makes new assumptions to force the given answer. This process yields MMathCoT-1M. The complete prompt designs can be found in Appendix G.

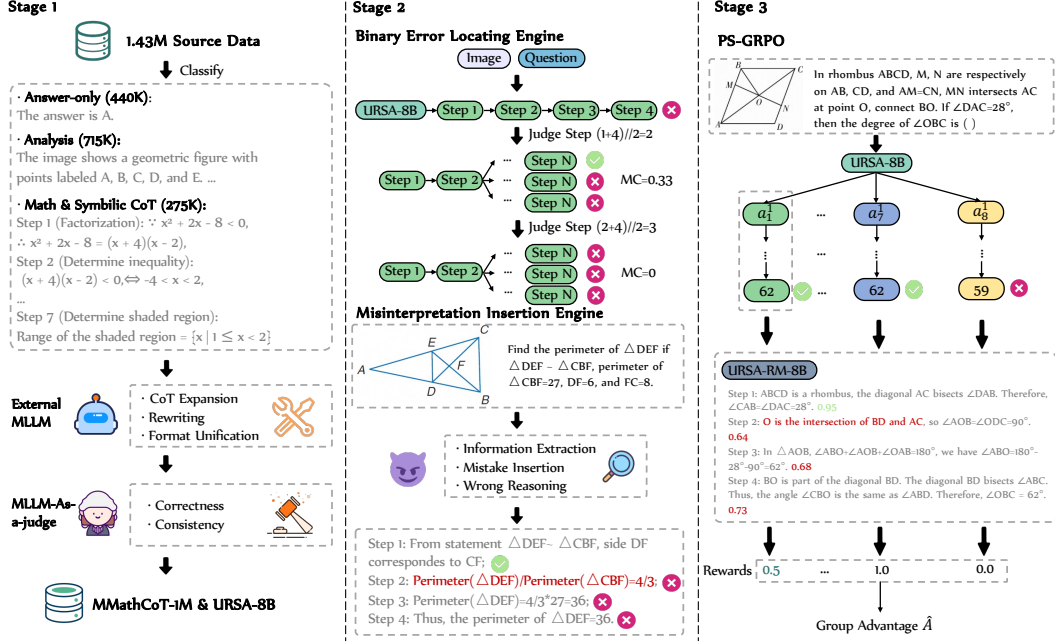


Figure 3: Pipeline of URSA. Stage 1 depicts the workflow of data curation as described in Section 2. Stage 2 illustrates how binary error locating and misinterpretation insertion facilitate the automation of process supervision data. Stage 3 demonstrates how our PS-GRPO operates by imposing penalties on rollouts that are questioned by the PRM.

We perform full-parameter instruction fine-tuning with MMathCoT-1M to train URSA-8B, based on the aligned model. The SFT dataset \mathcal{D}_{SFT} is formed by the union of the curated solutions, i.e., $\mathcal{D}_{SFT} = \{(x_i, y_i) \mid (x_i, y_i) \in \mathcal{S}_{Ao} \cup \mathcal{S}_{An} \cup \mathcal{S}_C\}$. Training objective is demonstrated in Equation 1.

$$\mathcal{L}_{SFT} = -\mathbb{E}_{(x, y) \sim \mathcal{D}_{SFT}} \sum_{t=1}^T \log \mathcal{M}(y_t | x, y_{<t}) \quad (1)$$

In this phase, we construct a stronger reasoning foundation model, URSA-8B, with the expectation of achieving a higher bound at inference time and to process supervision data of greater diversity.

3 Stage II: Dual-View Process Supervised Data Synthesis

3.1 Binary Error Locating Engine

Following suggestions by previous work [41–43], we train a PRM for first error step identification. We collect $\sim 553K$ incorrect solutions from URSA-8B’s zero-shot inference on MMathCoT-1M. Erroneous steps in these solutions are labeled using Monte Carlo Tree Search (MCTS). For MCTS, an operation $\mathcal{F}(\{s_1, \dots, s_i\}, N)$ generates N rollouts from a reasoning prefix $\{s_1, \dots, s_i\}$. The single step’s Monte Carlo estimation value, mc_i , is the fraction of these rollouts leading to a correct answer:

$$mc_i = \frac{|\text{Correct rollouts from } \mathcal{F}(\{s_1, s_2, \dots, s_i\}, N)|}{|\text{Total rollouts from } \mathcal{F}(\{s_1, s_2, \dots, s_i\}, N)|} \quad (2)$$

A step s_i is deemed “potentially correct” if $mc_i > 0$ [43, 42]. We optimize the identification of first error step using Binary Error Locating Engine (BEL): if the middle step has positive mc (i.e. $mc_{mid} > 0$), the error is in the latter half; otherwise, in the first (see Algorithm 1). To mitigate step-level label bias and include positive examples, we add $\sim 180K$ correct solutions (1/3 the number of incorrect ones), with all steps easily marked “True”. This yields \mathcal{S}_{BEL} , a 773K process annotation dataset based on correctness potential.

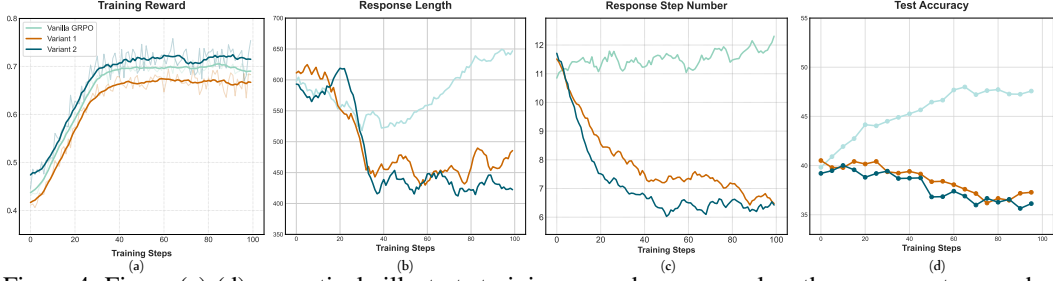


Figure 4: Figure (a)-(d) respectively illustrate training rewards, response length, response step number and test set accuracy of vanilla GRPO and two variants proposed in Section 4. Test set is randomly selected 500 examples from MMathCoT-1M for an in-domain evaluation.

3.2 Misinterpretation Insertion Engine

Apart from logical errors, the perception inconsistency between images and text in reasoning steps is a unique problem in multimodal scenarios [30, 44, 45]. We propose a Misinterpretation Insertion Engine (MIE) to artificially insert hallucinatory information, automatically constructing process supervision data with incorrect reasoning paths starting from the insertion point. Specifically, MIE includes three steps. First, we prompt \mathcal{G} to perform a captioning task, extracting mathematical paradigm information from the image as much as possible. Second, the model \mathcal{G} is required to focus on potentially confusable conditions within the existing correct solution and modify them using adjacent or similar conditions. Finally, the model \mathcal{G} is prompted to continue reasoning based on the step with the inserted error. We leverage strong instruction-following capability of \mathcal{G} , instructing it to automatically assign negative labels to every subsequent step following the erroneous insertion. We generate $\sim 302K$ samples \mathcal{S}_{MIE} using this strategy. Cases from MIE can be found in the Appendix H.2.

3.3 PRM Training

As shown in Equation 3, we merge two types of data, proposing a $\sim 1.1M$ process supervision data called DualMath-1.1M. During training, we append a special token after each step to indicate its predicted correctness. We model the PRM training as a binary classification task for the correctness of each step, as shown in Equation 4, here π_p is the trained PRM based on URSA-8B. e_j and y_j represent single step and corresponding label ($y_j \in \{0, 1\}$).

$$\mathcal{D}_{PRM} = \{(e, y_e) \sim \mathcal{S}_{BEL} \cup \mathcal{S}_{MIE}\} \quad (3)$$

$$\mathcal{L}_{PRM} = -\mathbb{E}_{(e,y) \sim \mathcal{D}_{PRM}} \sum_{j=1}^{|e|} \left[y_j \log \pi_p(e_j) + (1 - y_j) \log(1 - \pi_p(e_j)) \right] \quad (4)$$

Thus, Stage II delivers URSA-8B-RM, a strong PRM trained on DualMath-1.1M—the **first** large-scale, automatically labeled dataset for multimodal reasoning process supervision. While BoN evaluation demonstrates PRM’s value in TTS, a critical question emerges: how can its guidance be directly integrated into MLLM post-training? This remains largely uncharted. Stage III draws a lesson about why previous scalar process reward modeling tends to fail, and then we achieve effective progress through process-as-outcome reward modeling.

4 Stage III: Integrating multimodal PRM into RL

Inspired by successes like DeepSeek-R1 [46], several recent studies have tried to adapt outcome reward-based GRPO for multimodal reasoning, demonstrating notable progress [47–50]. Outcome reward-based GRPO computes the i -th response’s advantage through normalizing in-group rewards. However, outcome reward-based GRPO ignores the quality of reasoning processes [41, 51, 52].

Following most standard response-level and step-level reward modeling in RL [43, 28, 46, 13, 53], we examine two simple variants of GRPO with integrated scalar process rewards to reveal the failure patterns during the training process [54]. *Variant 1*: For i -th rollout, the reward is the sum of the

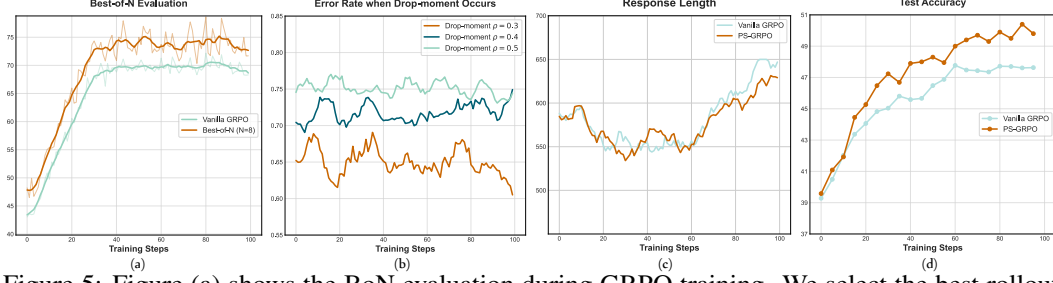


Figure 5: Figure (a) shows the BoN evaluation during GRPO training. We select the best rollout using the mean value of process rewards. Figure (b) illustrates the proportion of rollouts where URSA-8B-RM identifies “drop-moment” and the final results are indeed incorrect. Figures (c) and (d) display the response length and test accuracy during PS-GRPO training.

outcome reward and the average process reward, i.e. $r^i = r_o^i + \bar{r}_s^i$. *Variant 2*: Despite the outcome reward, a scalar process reward $r_{s,t}^i$ is assigned to the i -th rollout’s t -th step. We observe two highly significant conclusions from Figure 4: **(i) High susceptibility to reward hacking**. The test accuracy of both variants is lower than vanilla GRPO. This indicates that when process scalar rewards are employed as learning objectives, the model quickly learns strategies that cater to process correctness. However, correctness in the process does not necessarily correlate fully with the heuristics leading to the ground-truth. **(ii) PRM’s length bias in rewarding**. We observe a trend where increased training leads to shorter model responses and fewer reasoning steps. This phenomenon stems from an inherent length bias in the PRM’s training labels; for examples with incorrect answers, steps taken after the first error are unlikely to yield a correct solution. This results in the PRM conservatively rewards the later stages of a reasoning rollout, thereby encouraging the MLLM towards more passive reasoning and a reliance on pattern recognition from existing conditions or simpler heuristics.

PS-GRPO The findings above confirm the consideration that flaws in the reward function are amplified when scalar process rewards serve as the optimization target [55, 33]. We ask “Which internal signals of PRM can be trusted?” We employ two views to investigate the reliable region of the PRM: first, the BoN performance during online learning, and second, the PRM’s error identification capability. Regarding the latter, we introduce the concept of a “*drop-moment*” within the PRM’s reward sequence, which signifies that the PRM questions the validity of the preceding steps. Specifically, for a given solution’s PRM reward sequence $\{r_{p,1}^i, r_{p,2}^i, \dots, r_{p,N}^i\}$, a significant decrease in reward between consecutive steps indicates the occurrence of such a drop-moment.

$$\delta_p^i = \max \left\{ \frac{r_{p,j}^i - r_{p,j+1}^i}{r_{p,j}^i} \middle| j = 0, 1, \dots, N-1 \right\} > \rho \quad (5)$$

Here, ρ represents PRM’s drop-moment threshold. As illustrated in Figure 5, the PRM’s ability for BoN selection and error identification remains largely unimpaired during the online RL process, exhibiting stable performance. This suggests that *although the scalar reward from the PRM in online RL might be unreliable, the relative quality of solutions it reveals is comparatively trustworthy*.

We leverage this beneficial property to address the reward sparsity problem in GRPO [56–58], aiming to make online RL focus more on learning from rollouts that have accurate results and rigorous processes. We use ρ from Equation 5 as the occurrence threshold for a “*drop-moment*”; when it occurs, we apply a reward penalty γ to rollouts with correct results. This both differentiates the learning value of outcome-correct rollouts and, due to its focus on relative drops in reward sequences, circumvents the impact of PRM’s length bias in rewarding.

$$R^i = \begin{cases} 1, & o^i \text{ is correct and } \delta_p^i < \rho \\ 1 - \gamma, & o^i \text{ is correct and } \delta_p^i \geq \rho \\ 0, & \text{otherwise} \end{cases} \quad (6)$$

We utilize reward modeling in Equation 6 to conduct a process-supervised GRPO, which facilitates the computation of in-group advantages in Equation 7.

Table 1: Performance Comparison on 6 math reasoning benchmarks. We use accuracy for MathVerse, MathVision, MathVista and GeoQA. We use Score (Loose) on WE-MATH. And average-case accuracy is employed on DYNAMATH. Best results of Closed-source MLLMs are highlighted in green. Best and runner-up results of Open-source MLLMs are highlighted in red and blue.

	Size	Avg	MathVerse testmini	MathVision full set	MathVista gps	WE-MATH testmini	DYNAMATH testmini	GeoQA full set
<i>Closed-Source MLLMs</i>								
GPT-4o [59]	-	55.5	50.2	30.4	64.7	62.8	64.9	62.1
GPT-4o-mini [59]	-	49.2	42.3	22.8	59.9	56.3	53.5	60.1
Gemini-1.5-pro [60]	-	53.2	35.3	19.2	81.7	66.9	60.5	55.5
<i>Open-Source General MLLMs</i>								
InternVL-Chat-V1.5 [61]	26B	33.6	26.1	15.4	56.9	32.7	36.7	33.5
Llama-3.2-11B-Vision-Instruct [62]	11B	28.0	28.9	16.9	40.9	12.0	32.2	36.9
Qwen2-VL [63]	8B	40.2	33.6	19.2	51.0	43.0	42.1	52.2
InternVL2-8B [64]	8B	41.8	37.0	18.4	57.7	44.9	39.7	52.8
InternVL2-8B-MPO [65]	8B	45.1	38.2	22.3	69.2	44.4	40.5	55.9
InternVL2.5-8B [66]	8B	45.2	39.5	19.7	64.9	44.7	40.5	61.6
LLaVA-OneVision [35]	8B	40.9	28.9	18.3	71.6	44.9	37.5	43.9
Points-Qwen2.5-Instruct [67]	8B	49.8	41.1	23.9	76.0	51.0	42.8	63.8
Gemma3-12B [68]	12B	49.8	40.1	29.1	63.6	51.7	45.8	67.7
<i>Open-Source Reasoning MLLMs</i>								
Math-LLaVA [15]	13B	35.2	22.9	15.7	57.7	31.3	35.5	48.1
MathPUMA-Qwen2-7B [11]	8B	39.6	33.6	14.0	48.1	41.0	37.3	63.6
MultiMath [23]	7B	43.1	27.7	16.3	66.8	42.2	37.9	67.7
MAVIS [19]	7B	44.4	35.2	18.5	64.1	44.3	36.2	68.3
InfiMM-Math [14]	7B	48.6	40.5	18.8	77.3	48.3	38.2	68.3
AtomThink-EMOVA [12]	8B	49.5	42.5	24.9	75.9	49.3	40.9	63.8
MathGLM-Vision [9]	9B	47.6	44.2	19.2	64.2	45.2	42.2	70.4
LlamaV-o1 [69]	11B	38.4	33.9	17.9	53.3	42.6	34.7	43.1
OpenVLThinker [70]	7B	-	47.9	25.3	76.4	-	-	-
R1-Onevision [71]	7B	-	47.4	26.9	72.4	51.4	-	-
URSA-8B	8B	54.7	45.7	28.7	81.7	53.6	44.7	73.5
URSA-8B-PS-GRPO	8B	58.2	50.9	31.5	83.2	60.7	47.4	75.6

Table 2: Comparison of TTS on URSA-8B and AtomThink-EMOVA using BoN performance.

Model	Method	MathVerse				MathVista-GPS				MathVision			
		N=4	N=8	N=16	N=32	N=4	N=8	N=16	N=32	N=4	N=8	N=16	N=32
URSA-8B	Self-Consistency	49.3	50.1	50.7	50.7	82.7	83.9	84.8	85.4	29.4	31.9	32.8	33.1
	InternVL2.5-8B ORM	48.6	50.9	51.8	51.3	82.5	83.3	84.3	85.1	29.9	32.1	32.8	33.5
	URSA-8B-RM	53.3	54.2	54.7	55.0	83.2	85.5	86.5	87.2	31.6	33.1	34.0	35.1
AtomThink-EMOVA	Self-Consistency	45.9	46.7	47.1	47.3	76.8	77.9	78.6	79.0	25.3	26.8	27.6	28.0
	InternVL2.5-8B ORM	45.7	45.6	46.4	46.1	76.6	77.7	78.3	79.2	26.0	26.6	27.2	27.8
	URSA-8B-RM	48.0	48.8	49.3	49.6	78.0	79.6	80.5	81.0	27.5	29.0	30.2	31.0

5 Experiments

5.1 Experimental Setup

Benchmarks We evaluate our URSA-series models on 6 widely used reasoning benchmarks, including MathVerse [72], DYNAMATH [73], MathVista [74], WE-MATH [75], GeoQA [40] and MathVision [43]. Detailed description and evaluation criteria can be found in Appendix F.3. We consistently employ zero-shot inference for comparison.

Baselines We include some leading proprietary MLLMs, such as GPT-4o and GPT-4o-mini [59]. For open-source MLLMs with comparable size, we select InternVL-series [64, 76], LLaVA-OneVision [35], Gemma3-12B [68], Qwen2-VL [63], and so on. For MLLMs intended for math reasoning purposes, we select AtomThink [12], InfiMM-Math [14], MAVIS [19], MathGLM-Vision [9], LlamaV-o1 [69]. This kind of work focuses on the synthesis of STEM reasoning data or o1-like slow thinking. We do not select baselines that use MathVision as training set for fairness, such as Mulberry-Qwen2-VL-7B [77] and MAMooTH-VL [78]. For PRM’s TTS performance, we select Self-Consistency [79] and open-source MLLM as ORM for comparison, such as InternVL2.5-8B [64].

Implementation Details URSA uses SAM-B+SigLIP-L as the hybrid vision encoder and Qwen2.5-Math-Instruct as the LLM backbone. We employ a two-layer MLP connection for vision-language alignment training. We select 15K data in MMathCoT-1M for PS-GRPO. γ and ρ in Equation 6 are

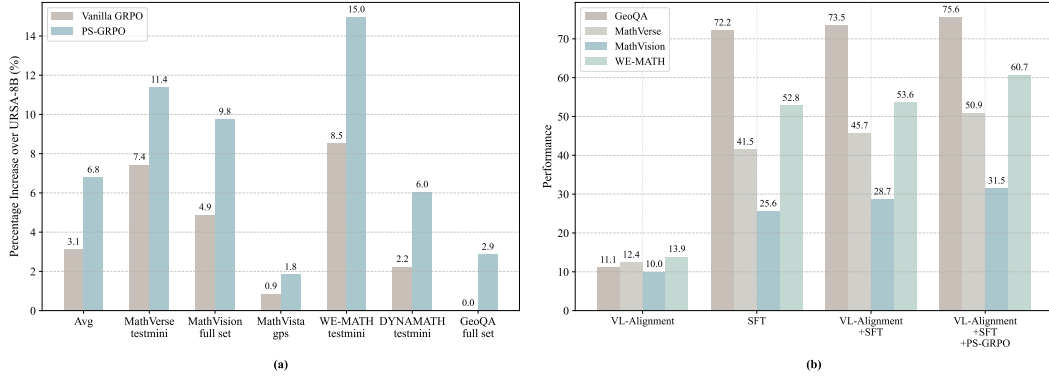


Figure 6: Figure(a) represents the comparison of relative improvements on URSA-8B; Figure(b) illustrates how each training stage contributes to the total performance.

set to 0.5 and 0.3, respectively. Details on module selection, data selection, hyperparameters, and time cost are placed in the Appendix D and F.

5.2 Main Results

SoTA Performance In Table 1, we present the performance of URSA-8B and URSA-8B-PS-GRPO. First, URSA-8B provides a stronger reasoning foundation model. It demonstrates a 5.2 point advantage over AtomThink-EMOVA which focuses on “slow thinking” training. It also outperforms leading general-purpose MLLMs of comparable size, such as Gemma3-12B and InternVL2.5-8B. URSA-8B-PS-GRPO outperforms GPT-4o across 6 benchmarks on average and shows significant advantages on MathVista-GPS (83.2 vs 62.6), GeoQA (73.5 vs 62.1), and achieves the first surpassing performance on MathVision (31.5 vs 30.4). However, a significant performance gap on DynaMath suggests that smaller-scale MLLMs still lack more robust problem-solving capabilities. Compared to the leading math reasoning MLLM AtomThink-EMOVA-8B and general-purpose MLLM Gemma3-12B in terms of average performance, our model shows advantages of **8.5%** and **8.2%**, respectively. Compared with recent R1-inspired method OpenVLThinker [70] and R1-Onevision [71], we still show significant advantage on MathVision and WE-MATH.

Effective Best-of-N Evaluation In Table 2, we demonstrate the advantages of URSA-8B-RM compared to self-consistency and the ORM baseline on serving TTS [43, 42]. We find that self-consistency remains a strong baseline, which InternVL2.5-8B (serving as the ORM) does not consistently surpasses. However, URSA-8B-RM exhibits more effective BoN evaluation and demonstrates its generalization on AtomThink-EMOVA-8B. In addition, using URSA-8B-RM as the verifier, only 4 samplings can achieve a huge improvement based on URSA-8B. Specifically, it provides a 16.6% and 10.1% relative improvement on MathVerse and MathVision. In Best-of-32 setting, URSA-8B achieve 35.1 and 55.0 in MathVision and MathVerse, showing clear advantage with GPT-4o.

PS-GRPO vs Vanilla GRPO As shown in Figure 6 (a), given the same training data, hyperparameters, and rollout number PS-GRPO achieves a higher improvement on average performance (6.8% vs 3.1%). PS-GRPO demonstrates an improvement that is nearly double that of vanilla GRPO in WE-MATH and more challenging MathVision, suggesting its effectiveness. We notice that the improvement of RL on MathVista-GPS and GeoQA is relatively small. This is because URSA-8B’s inherent abilities have already achieved an effect close to the upper bound on these two benchmarks. However, PS-GRPO still has advantages over vanilla GRPO.

6 Analysis

6.1 How Each Stage Contributes the Performance

In this section, we demonstrate how each stage contributes to the performance. As demonstrated in Figure 6 (b), all stages make a performance contribution. MMathCoT-1M contributes the highest absolute performance gain. The effect of Alignment-860K is more evident on MathVerse and MathVision,

Table 3: Ablation study on DualMath-1.1M (BoN evaluation). w/o \mathcal{S}_{MIE} and w/o \mathcal{S}_{BEL} represents dropping one part of DualMath-1.1M to train the PRM.

Model	Dataset	MathVerse				MathVista-GPS				MathVision			
		N=4	N=8	N=16	N=32	N=4	N=8	N=16	N=32	N=4	N=8	N=16	N=32
URSA-8B	DualMath-1.1M	53.3	54.2	54.7	55.0	83.2	85.5	86.5	87.2	31.6	33.1	34.0	35.1
	w/o \mathcal{S}_{MIE}	52.8	52.6	52.4	53.9	81.3	83.8	83.1	83.2	29.9	30.5	33.1	34.5
	w/o \mathcal{S}_{BEL}	50.3	51.4	51.8	53.0	80.1	83.1	82.2	83.0	28.7	29.8	32.3	34.2
AtomThink-EMOVA	DualMath-1.1M	48.0	48.8	49.3	49.6	78.0	79.6	80.5	81.0	27.5	29.0	30.2	31.0
	w/o \mathcal{S}_{MIE}	47.5	48.2	47.8	48.0	76.8	78.3	79.1	79.5	26.0	27.4	28.5	29.2
	w/o \mathcal{S}_{BEL}	46.8	47.5	47.9	47.3	76.0	77.5	78.3	78.7	25.4	26.7	27.8	28.5

Table 4: Sensitivity analysis on reward penalty and PRM’s “drop-moment” judgment.

γ	ρ	MathVerse testmini	MathVision full set	MathVista gps	WE-MATH testmini	DYNAMATH testmini	GeoQA full set	Avg
0.5	0.3	50.9	31.5	83.2	60.7	47.4	75.6	58.2
0.5	0.4	49.9	30.8	81.2	59.9	46.9	75.0	57.3
0.5	0.2	49.6	30.5	80.9	59.6	46.6	74.7	57.0
1.0	0.3	49.0	29.4	79.8	58.8	45.3	72.5	56.3
0.7	0.3	52.0	31.1	81.7	59.6	47.0	73.8	57.5
0.3	0.3	51.5	32.0	82.1	61.0	46.3	74.6	57.9

likely because the question images in these two datasets contain richer textual modality information, allowing alignment resources (such as textual images) to better supplement this comprehension capability. PS-GRPO, on the other hand, is dedicated to breaking the bottleneck after large-scale SFT, performing more prominently on WE-MATH and MathVerse with relative improvements of 13.2% and 11.4% respectively, compared to URSA-8B. We provide a generalization validation on InternVL2.5-8B and Multimath in Appendix C.4.

6.2 Ablation Studies on Automatic Process Labeling

We give an ablation study on how two parts of DualMath-1.1M contribute to URSA-8B-RM. As shown in Table 3, we can see that the method based on BEL, which focuses on the potential to correctness, and the method based on MIE, which focuses on the perception consistency, both contribute positively to the outcome. This further illustrates that in the process of multimodal math reasoning, image-text inconsistency is widespread and needs to be mitigated. We address this issue by augmenting the process supervision training data through the enforced imposition of common hallucination categories. Specifically, the data generated by BEL demonstrates a more significant impact, indicating that the quality of synthesized data can still be improved.

6.3 Sensitivity Analysis on Reward Penalty and Drop-moment

In this section, we conduct a sensitivity analysis on two hyperparameters of PS-GRPO, γ and ρ . These respectively define the magnitude of the reward penalty for rollouts exhibiting a “drop-moment” and the tolerance threshold for identifying such “drop-moments”. As shown in Table 4, our core findings are twofold: (i) The value of γ should not be set too high, as this implies excessive trust in the PRM, which may cause the rewards of a group to vanish and lead to training instability. When fixing ρ at 0.3, we find that setting γ to a value within a certain appropriate range (we test 0.3-0.7) is generally beneficial for average performance. (ii) An excessively large ρ diminishes reward differentiation, causing the RL behavior to approximate that of vanilla GRPO. Conversely, an excessively small ρ is unreasonable by design, as it is overly sensitive to process reward changes and tends to result in an overly broad range of penalties. In an extreme case where all correct rollouts are penalized, PS-GRPO degenerates back to vanilla GRPO.

7 Conclusion

In this study, we take the first step to thoroughly explore the application of PRM in multimodal math reasoning. We introduce a three-stage training pipeline URSA designed to address three major

challenges. Initially, we provide a large-scale CoT reasoning dataset MMathCoT-1M. This dataset forms the basis for developing URSA-8B, a MLLM with enhanced reasoning capabilities, and paves the way for further TTS or RL scenarios. Next, we present a dual-view automated process supervision annotation method, covering logical validity and perceptual consistency in multimodal scenarios. We introduce the first large-scale process supervision dataset in multimodal reasoning, DualMath-1.1M. Finally, we address reward hacking and rewarding length bias through process-as-outcome modeling, and put forward PS-GRPO, which is a PRM-aided online RL method that surpasses GRPO. The resulting URSA-8B-PS-GRPO model demonstrates superior average performance over leading open-source MLLM such as Gemma3-12B (8.4%) and proprietary GPT-4o (2.7%).

References

- [1] Haipeng Luo, Qingfeng Sun, Can Xu, Pu Zhao, Jianguang Lou, Chongyang Tao, Xiubo Geng, Qingwei Lin, Shifeng Chen, and Dongmei Zhang. Wizardmath: Empowering mathematical reasoning for large language models via reinforced evol-instruct. *arXiv preprint arXiv:2308.09583*, 2023.
- [2] An Yang, Beichen Zhang, Binyuan Hui, Bofei Gao, Bowen Yu, Chengpeng Li, Dayiheng Liu, Jianhong Tu, Jingren Zhou, Junyang Lin, Keming Lu, Mingfeng Xue, Runji Lin, Tianyu Liu, Xingzhang Ren, and Zhenru Zhang. Qwen2.5-math technical report: Toward mathematical expert model via self-improvement. *CoRR*, abs/2409.12122, 2024. doi: 10.48550/ARXIV.2409.12122. URL <https://doi.org/10.48550/arXiv.2409.12122>.
- [3] Huaiyuan Ying, Shuo Zhang, Linyang Li, Zhejian Zhou, Yunfan Shao, Zhaoye Fei, Yichuan Ma, Jiawei Hong, Kuikun Liu, Ziyi Wang, Yudong Wang, Zijian Wu, Shuaibin Li, Fengzhe Zhou, Hongwei Liu, Songyang Zhang, Wenwei Zhang, Hang Yan, Xipeng Qiu, Jiayu Wang, Kai Chen, and Dahua Lin. Internlm-math: Open math large language models toward verifiable reasoning. *CoRR*, abs/2402.06332, 2024. doi: 10.48550/ARXIV.2402.06332. URL <https://doi.org/10.48550/arXiv.2402.06332>.
- [4] Zhihong Shao, Peiyi Wang, Qihao Zhu, Runxin Xu, Junxiao Song, Xiao Bi, Huawei Zhang, Mingchuan Zhang, YK Li, Y Wu, et al. Deepseekmath: Pushing the limits of mathematical reasoning in open language models. *arXiv preprint arXiv:2402.03300*, 2024.
- [5] Zhen Yang, Jinhao Chen, Zhengxiao Du, Wenmeng Yu, Weihan Wang, Wenyi Hong, Zhihuan Jiang, Bin Xu, Yuxiao Dong, and Jie Tang. Mathglm-vision: Solving mathematical problems with multi-modal large language model. *arXiv preprint arXiv:2409.13729*, 2024.
- [6] Longhui Yu, Weisen Jiang, Han Shi, Jincheng Yu, Zhengying Liu, Yu Zhang, James T. Kwok, Zhengu Li, Adrian Weller, and Weiyang Liu. Metamath: Bootstrap your own mathematical questions for large language models. In *The Twelfth International Conference on Learning Representations, ICLR 2024, Vienna, Austria, May 7-11, 2024*. OpenReview.net, 2024. URL <https://openreview.net/forum?id=N8N0hgNDrt>.
- [7] Xinzhe Ni, Yeyun Gong, Zhibin Gou, Yelong Shen, Yujiu Yang, Nan Duan, and Weizhu Chen. Exploring the mystery of influential data for mathematical reasoning. *CoRR*, abs/2404.01067, 2024. doi: 10.48550/ARXIV.2404.01067. URL <https://doi.org/10.48550/arXiv.2404.01067>.
- [8] Yiyao Yu, Yuxiang Zhang, Dongdong Zhang, Xiao Liang, Hengyuan Zhang, Xingxing Zhang, Ziyi Yang, Mahmoud Khademi, Hany Awadalla, Junjie Wang, Yujiu Yang, and Furu Wei. Chain-of-reasoning: Towards unified mathematical reasoning in large language models via a multi-paradigm perspective. *CoRR*, abs/2501.11110, 2025. doi: 10.48550/ARXIV.2501.11110. URL <https://doi.org/10.48550/arXiv.2501.11110>.
- [9] Zhen Yang, Jinhao Chen, Zhengxiao Du, Wenmeng Yu, Weihan Wang, Wenyi Hong, Zhihuan Jiang, Bin Xu, Yuxiao Dong, and Jie Tang. Mathglm-vision: Solving mathematical problems with multi-modal large language model. *CoRR*, abs/2409.13729, 2024. doi: 10.48550/ARXIV.2409.13729. URL <https://doi.org/10.48550/arXiv.2409.13729>.
- [10] Huanjin Yao, Jiaxing Huang, Wenhao Wu, Jingyi Zhang, Yibo Wang, Shunyu Liu, Yingjie Wang, Yuxin Song, Haocheng Feng, Li Shen, and Dacheng Tao. Mulberry: Empowering MLLM with o1-like reasoning and reflection via collective monte carlo tree search. *CoRR*, abs/2412.18319, 2024. doi: 10.48550/ARXIV.2412.18319. URL <https://doi.org/10.48550/arXiv.2412.18319>.
- [11] Wenwen Zhuang, Xin Huang, Xiantao Zhang, and Jin Zeng. Math-puma: Progressive upward multimodal alignment to enhance mathematical reasoning. In *Proceedings of the AAAI Conference on Artificial Intelligence*, volume 39, pages 26183–26191, 2025.

[12] Kun Xiang, Zhili Liu, Zihao Jiang, Yunshuang Nie, Runhui Huang, Haoxiang Fan, Hanhui Li, Weiran Huang, Yihan Zeng, Jianhua Han, et al. Atomthink: A slow thinking framework for multimodal mathematical reasoning. *arXiv preprint arXiv:2411.11930*, 2024.

[13] Wenxuan Huang, Bohan Jia, Zijie Zhai, Shaosheng Cao, Zheyu Ye, Fei Zhao, Zhe Xu, Yao Hu, and Shaohui Lin. Vision-r1: Incentivizing reasoning capability in multimodal large language models. *CoRR*, abs/2503.06749, 2025. doi: 10.48550/ARXIV.2503.06749. URL <https://doi.org/10.48550/arXiv.2503.06749>.

[14] Xiaotian Han, Yiren Jian, Xuefeng Hu, Haogeng Liu, Yiqi Wang, Qihang Fan, Yuang Ai, Huaibo Huang, Ran He, Zhenheng Yang, et al. Infimm-webmath-40b: Advancing multimodal pre-training for enhanced mathematical reasoning. In *The 4th Workshop on Mathematical Reasoning and AI at NeurIPS’24*, 2024.

[15] Wenhao Shi, Zhiqiang Hu, Yi Bin, Junhua Liu, Yang Yang, See-Kiong Ng, Lidong Bing, and Roy Ka-Wei Lee. Math-llava: Bootstrapping mathematical reasoning for multimodal large language models. *arXiv preprint arXiv:2406.17294*, 2024.

[16] Shihao Cai, Keqin Bao, Hangyu Guo, Jizhi Zhang, Jun Song, and Bo Zheng. Geogpt4v: Towards geometric multi-modal large language models with geometric image generation. *arXiv preprint arXiv:2406.11503*, 2024.

[17] Linger Deng, Yuliang Liu, Bohan Li, Dongliang Luo, Liang Wu, Chengquan Zhang, Pengyuan Lyu, Ziyang Zhang, Gang Zhang, Errui Ding, et al. R-cot: Reverse chain-of-thought problem generation for geometric reasoning in large multimodal models. *arXiv preprint arXiv:2410.17885*, 2024.

[18] Jiahui Gao, Renjie Pi, Jipeng Zhang, Jiacheng Ye, Wanjun Zhong, Yufei Wang, Lanqing Hong, Jianhua Han, Hang Xu, Zhenguo Li, and Lingpeng Kong. G-llava: Solving geometric problem with multi-modal large language model. *CoRR*, abs/2312.11370, 2023. doi: 10.48550/ARXIV.2312.11370. URL <https://doi.org/10.48550/arXiv.2312.11370>.

[19] Renrui Zhang, Xinyu Wei, Dongzhi Jiang, Ziyu Guo, Shicheng Li, Yichi Zhang, Chengzhuo Tong, Jiaming Liu, Aojun Zhou, Bin Wei, et al. Mavis: Mathematical visual instruction tuning with an automatic data engine. *arXiv preprint arXiv:2407.08739*, 2024.

[20] Renqiu Xia, Mingsheng Li, Hancheng Ye, Wenjie Wu, Hongbin Zhou, Jiakang Yuan, Tianshuo Peng, Xinyu Cai, Xiangchao Yan, Bin Wang, Conghui He, Botian Shi, Tao Chen, Junchi Yan, and Bo Zhang. Geox: Geometric problem solving through unified formalized vision-language pre-training. *CoRR*, abs/2412.11863, 2024. doi: 10.48550/ARXIV.2412.11863. URL <https://doi.org/10.48550/arXiv.2412.11863>.

[21] Renqiu Xia, Bo Zhang, Hancheng Ye, Xiangchao Yan, Qi Liu, Hongbin Zhou, Zijun Chen, Min Dou, Botian Shi, Junchi Yan, and Yu Qiao. Chartx & chartvlm: A versatile benchmark and foundation model for complicated chart reasoning. *CoRR*, abs/2402.12185, 2024. doi: 10.48550/ARXIV.2402.12185. URL <https://doi.org/10.48550/arXiv.2402.12185>.

[22] Zhuosheng Zhang, Aston Zhang, Mu Li, Hai Zhao, George Karypis, and Alex Smola. Multimodal chain-of-thought reasoning in language models. *Trans. Mach. Learn. Res.*, 2024, 2024. URL <https://openreview.net/forum?id=y1pPWFVfvR>.

[23] Shuai Peng, Di Fu, Liangcai Gao, Xiuqin Zhong, Hongguang Fu, and Zhi Tang. Multimath: Bridging visual and mathematical reasoning for large language models. *arXiv preprint arXiv:2409.00147*, 2024.

[24] Ruohong Zhang, Bowen Zhang, Yanghao Li, Haotian Zhang, Zhiqing Sun, Zhe Gan, Yinfei Yang, Ruoming Pang, and Yiming Yang. Improve vision language model chain-of-thought reasoning. *arXiv preprint arXiv:2410.16198*, 2024.

[25] Runze Liu, Junqi Gao, Jian Zhao, Kaiyan Zhang, Xiu Li, Biqing Qi, Wanli Ouyang, and Bowen Zhou. Can 1b LLM surpass 405b ILM? rethinking compute-optimal test-time scaling. *CoRR*, abs/2502.06703, 2025. doi: 10.48550/ARXIV.2502.06703. URL <https://doi.org/10.48550/arXiv.2502.06703>.

[26] Lunjun Zhang, Arian Hosseini, Hritik Bansal, Mehran Kazemi, Aviral Kumar, and Rishabh Agarwal. Generative verifiers: Reward modeling as next-token prediction. *arXiv preprint arXiv:2408.15240*, 2024.

[27] Dan Zhang, Sining Zhoubian, Ziniu Hu, Yisong Yue, Yuxiao Dong, and Jie Tang. Rest-mcts*: LLM self-training via process reward guided tree search. In Amir Globersons, Lester Mackey, Danielle Belgrave, Angela Fan, Ulrich Paquet, Jakub M. Tomczak, and Cheng Zhang, editors, *Advances in Neural Information Processing Systems 38: Annual Conference on Neural Information Processing Systems 2024, NeurIPS 2024, Vancouver, BC, Canada, December 10 - 15, 2024*, 2024. URL http://papers.nips.cc/paper_files/paper/2024/hash/76ec4dc30e9faaf0e4b6093eaa377218-Abstract-Conference.html.

[28] Wei Liu, Junlong Li, Xiwen Zhang, Fan Zhou, Yu Cheng, and Junxian He. Diving into self-evolving training for multimodal reasoning. *CoRR*, abs/2412.17451, 2024. doi: 10.48550/ARXIV.2412.17451. URL <https://doi.org/10.48550/arXiv.2412.17451>.

[29] Yang Yue, Zhiqi Chen, Rui Lu, Andrew Zhao, Zhaokai Wang, Yang Yue, Shiji Song, and Gao Huang. Does reinforcement learning really incentivize reasoning capacity in llms beyond the base model? *arXiv preprint arXiv:2504.13837*, 2025.

[30] Yibo Yan, Shen Wang, Jiahao Huo, Hang Li, Boyan Li, Jiamin Su, Xiong Gao, Yi-Fan Zhang, Tianlong Xu, Zhendong Chu, et al. Errroradar: Benchmarking complex mathematical reasoning of multimodal large language models via error detection. *arXiv preprint arXiv:2410.04509*, 2024.

[31] Di Zhang, Jingdi Lei, Junxian Li, Xunzhi Wang, Yujie Liu, Zonglin Yang, Jiatong Li, Weida Wang, Suorong Yang, Jianbo Wu, et al. Critic-v: Vlm critics help catch vlm errors in multimodal reasoning. *arXiv preprint arXiv:2411.18203*, 2024.

[32] Jiaxin Ai, Pengfei Zhou, Zhaopan Xu, Ming Li, Fanrui Zhang, Zizhen Li, Jianwen Sun, Yukang Feng, Baojin Huang, Zhongyuan Wang, and Kaipeng Zhang. Projudge: A multi-modal multi-discipline benchmark and instruction-tuning dataset for mllm-based process judges. *CoRR*, abs/2503.06553, 2025. doi: 10.48550/ARXIV.2503.06553. URL <https://doi.org/10.48550/arXiv.2503.06553>.

[33] Lilian Weng. Reward hacking and how to mitigate it. <https://lilianweng.github.io/posts/2024-11-28-reward-hacking/>, November 2024. [Accessed 11-28-2024].

[34] Jiayi Fu, Xuandong Zhao, Chengyuan Yao, Heng Wang, Qi Han, and Yanghua Xiao. Reward shaping to mitigate reward hacking in RLHF. *CoRR*, abs/2502.18770, 2025. doi: 10.48550/ARXIV.2502.18770. URL <https://doi.org/10.48550/arXiv.2502.18770>.

[35] Bo Li, Yuanhan Zhang, Dong Guo, Renrui Zhang, Feng Li, Hao Zhang, Kaichen Zhang, Peiyuan Zhang, Yanwei Li, Ziwei Liu, et al. Llava-onevision: Easy visual task transfer. *arXiv preprint arXiv:2408.03326*, 2024.

[36] Xiaohua Zhai, Basil Mustafa, Alexander Kolesnikov, and Lucas Beyer. Sigmoid loss for language image pre-training. In *Proceedings of the IEEE/CVF International Conference on Computer Vision*, pages 11975–11986, 2023.

[37] Alexander Kirillov, Eric Mintun, Nikhila Ravi, Hanzi Mao, Chloe Rolland, Laura Gustafson, Tete Xiao, Spencer Whitehead, Alexander C Berg, Wan-Yen Lo, et al. Segment anything. In *Proceedings of the IEEE/CVF International Conference on Computer Vision*, pages 4015–4026, 2023.

[38] Haoyu Lu, Wen Liu, Bo Zhang, Bingxuan Wang, Kai Dong, Bo Liu, Jingxiang Sun, Tongzheng Ren, Zhuoshu Li, Hao Yang, et al. Deepseek-vl: towards real-world vision-language understanding. *arXiv preprint arXiv:2403.05525*, 2024.

[39] Trieu H Trinh, Yuhuai Wu, Quoc V Le, He He, and Thang Luong. Solving olympiad geometry without human demonstrations. *Nature*, 625(7995):476–482, 2024.

[40] Jiaqi Chen, Jianheng Tang, Jinghui Qin, Xiaodan Liang, Lingbo Liu, Eric Xing, and Liang Lin. Geoqa: A geometric question answering benchmark towards multimodal numerical reasoning. In *Findings of the Association for Computational Linguistics: ACL-IJCNLP 2021*, pages 513–523, 2021.

[41] Hunter Lightman, Vineet Kosaraju, Yura Burda, Harri Edwards, Bowen Baker, Teddy Lee, Jan Leike, John Schulman, Ilya Sutskever, and Karl Cobbe. Let's verify step by step. *arXiv preprint arXiv:2305.20050*, 2023.

[42] Liangchen Luo, Yinxiao Liu, Rosanne Liu, Samrat Phatale, Harsh Lara, Yunxuan Li, Lei Shu, Yun Zhu, Lei Meng, Jiao Sun, et al. Improve mathematical reasoning in language models by automated process supervision. *arXiv preprint arXiv:2406.06592*, 2024.

[43] Peiyi Wang, Lei Li, Zhihong Shao, Runxin Xu, Damai Dai, Yifei Li, Deli Chen, Yu Wu, and Zhifang Sui. Math-shepherd: Verify and reinforce llms step-by-step without human annotations. In *Proceedings of the 62nd Annual Meeting of the Association for Computational Linguistics (Volume 1: Long Papers)*, pages 9426–9439, 2024.

[44] Haojie Zheng, Tianyang Xu, Hanchi Sun, Shu Pu, Ruoxi Chen, and Lichao Sun. Thinking before looking: Improving multimodal llm reasoning via mitigating visual hallucination. *arXiv preprint arXiv:2411.12591*, 2024.

[45] Luyu Gao, Aman Madaan, Shuyan Zhou, Uri Alon, Pengfei Liu, Yiming Yang, Jamie Callan, and Graham Neubig. Pal: Program-aided language models. In *International Conference on Machine Learning*, pages 10764–10799. PMLR, 2023.

[46] Daya Guo, Dejian Yang, Haowei Zhang, Junxiao Song, Ruoyu Zhang, Runxin Xu, Qihao Zhu, Shirong Ma, Peiyi Wang, Xiao Bi, et al. Deepseek-r1: Incentivizing reasoning capability in llms via reinforcement learning. *arXiv preprint arXiv:2501.12948*, 2025.

[47] Jiazheng Pan, Che Liu, Junde Wu, Fenglin Liu, Jiayuan Zhu, Hongwei Bran Li, Chen Chen, Cheng Ouyang, and Daniel Rueckert. Medvilm-r1: Incentivizing medical reasoning capability of vision-language models (vlms) via reinforcement learning. *CoRR*, abs/2502.19634, 2025. doi: 10.48550/ARXIV.2502.19634. URL <https://doi.org/10.48550/arXiv.2502.19634>.

[48] Yufei Zhan, Yousong Zhu, Shurong Zheng, Hongyin Zhao, Fan Yang, Ming Tang, and Jinqiao Wang. Vision-r1: Evolving human-free alignment in large vision-language models via vision-guided reinforcement learning. *CoRR*, abs/2503.18013, 2025. doi: 10.48550/ARXIV.2503.18013. URL <https://doi.org/10.48550/arXiv.2503.18013>.

[49] Wenxuan Huang, Bohan Jia, Zijie Zhai, Shaosheng Cao, Zheyu Ye, Fei Zhao, Zhe Xu, Yao Hu, and Shaohui Lin. Vision-r1: Incentivizing reasoning capability in multimodal large language models. *CoRR*, abs/2503.06749, 2025. doi: 10.48550/ARXIV.2503.06749. URL <https://doi.org/10.48550/arXiv.2503.06749>.

[50] Xiangyan Liu, Jinjie Ni, Zijian Wu, Chao Du, Longxu Dou, Haonan Wang, Tianyu Pang, and Michael Qizhe Shieh. Noisyrollout: Reinforcing visual reasoning with data augmentation, 2025. URL <https://arxiv.org/abs/2504.13055>.

[51] Wendi Li and Yixuan Li. Process reward model with q-value rankings. *CoRR*, abs/2410.11287, 2024. doi: 10.48550/ARXIV.2410.11287. URL <https://doi.org/10.48550/arXiv.2410.11287>.

[52] Amrith Setlur, Chirag Nagpal, Adam Fisch, Xinyang Geng, Jacob Eisenstein, Rishabh Agarwal, Alekh Agarwal, Jonathan Berant, and Aviral Kumar. Rewarding progress: Scaling automated process verifiers for LLM reasoning. *CoRR*, abs/2410.08146, 2024. doi: 10.48550/ARXIV.2410.08146. URL <https://doi.org/10.48550/arXiv.2410.08146>.

[53] Yiran Ma, Zui Chen, Tianqiao Liu, Mi Tian, Zhuo Liu, Zitao Liu, and Weiqi Luo. What are step-level reward models rewarding? counterintuitive findings from mcts-boosted mathematical reasoning. In Toby Walsh, Julie Shah, and Zico Kolter, editors, *AAAI-25, Sponsored by the Association for the Advancement of Artificial Intelligence, February 25 - March 4, 2025, Philadelphia, PA, USA*, pages 24812–24820. AAAI Press, 2025. doi: 10.1609/AAAI.V39I23.34663. URL <https://doi.org/10.1609/aaai.v39i23.34663>.

[54] Jiaxuan Gao, Shusheng Xu, Wenjie Ye, Weilin Liu, Chuyi He, Wei Fu, Zhiyu Mei, Guangju Wang, and Yi Wu. On designing effective RL reward at training time for LLM reasoning. *CoRR*, abs/2410.15115, 2024. doi: 10.48550/ARXIV.2410.15115. URL <https://doi.org/10.48550/arXiv.2410.15115>.

[55] Dario Amodei, Chris Olah, Jacob Steinhardt, Paul Christiano, John Schulman, and Dan Mané. Concrete problems in ai safety. *arXiv preprint arXiv:1606.06565*, 2016.

[56] Jixiao Zhang and Chunsheng Zuo. Grpo-lead: A difficulty-aware reinforcement learning approach for concise mathematical reasoning in language models. *arXiv preprint arXiv:2504.09696*, 2025.

[57] Jingyi Zhang, Jiaxing Huang, Huanjin Yao, Shunyu Liu, Xikun Zhang, Shijian Lu, and Dacheng Tao. R1-vl: Learning to reason with multimodal large language models via step-wise group relative policy optimization. *arXiv preprint arXiv:2503.12937*, 2025.

[58] Qiying Yu, Zheng Zhang, Ruofei Zhu, Yufeng Yuan, Xiaochen Zuo, Yu Yue, Tiantian Fan, Gaohong Liu, Lingjun Liu, Xin Liu, et al. Dapo: An open-source llm reinforcement learning system at scale. *arXiv preprint arXiv:2503.14476*, 2025.

[59] OpenAI. GPT-4o system card, 2024. URL <https://openai.com/research/gpt-4o-system-card>.

[60] Gemini Team, Rohan Anil, Sebastian Borgeaud, Jean-Baptiste Alayrac, Jiahui Yu, Radu Soricut, Johan Schalkwyk, Andrew M Dai, Anja Hauth, Katie Millican, et al. Gemini: a family of highly capable multimodal models. *arXiv preprint arXiv:2312.11805*, 2023.

[61] Zhe Chen, Weiyun Wang, Hao Tian, Shenglong Ye, Zhangwei Gao, Erfei Cui, Wenwen Tong, Kongzhi Hu, Jiapeng Luo, Zheng Ma, et al. How far are we to gpt-4v? closing the gap to commercial multimodal models with open-source suites. *arXiv preprint arXiv:2404.16821*, 2024.

[62] Meta. Llama 3.2: Revolutionizing edge AI and vision with open, customizable models — ai.meta.com. <https://ai.meta.com/blog/llama-3-2-connect-2024-vision-edge-mobile-devices/>, 2024. [Accessed 17-04-2025].

[63] Peng Wang, Shuai Bai, Sinan Tan, Shijie Wang, Zhihao Fan, Jinze Bai, Keqin Chen, Xuejing Liu, Jialin Wang, Wenbin Ge, et al. Qwen2-vl: Enhancing vision-language model’s perception of the world at any resolution. *arXiv preprint arXiv:2409.12191*, 2024.

[64] Zhe Chen, Jiannan Wu, Wenhui Wang, Weijie Su, Guo Chen, Sen Xing, Muyan Zhong, Qinglong Zhang, Xizhou Zhu, Lewei Lu, et al. Internvl: Scaling up vision foundation models and aligning for generic visual-linguistic tasks. In *Proceedings of the IEEE/CVF Conference on Computer Vision and Pattern Recognition*, pages 24185–24198, 2024.

[65] Weiyun Wang, Zhe Chen, Wenhui Wang, Yue Cao, Yangzhou Liu, Zhangwei Gao, Jinguo Zhu, Xizhou Zhu, Lewei Lu, Yu Qiao, et al. Enhancing the reasoning ability of multimodal large language models via mixed preference optimization. *arXiv preprint arXiv:2411.10442*, 2024.

[66] Zhe Chen, Weiyun Wang, Yue Cao, Yangzhou Liu, Zhangwei Gao, Erfei Cui, Jinguo Zhu, Shenglong Ye, Hao Tian, Zhaoyang Liu, et al. Expanding performance boundaries of open-source multimodal models with model, data, and test-time scaling. *arXiv preprint arXiv:2412.05271*, 2024.

[67] Yuan Liu, Zhongyin Zhao, Ziyuan Zhuang, Le Tian, Xiao Zhou, and Jie Zhou. Points: Improving your vision-language model with affordable strategies. *arXiv preprint arXiv:2409.04828*, 2024.

[68] Gemma Team, Aishwarya Kamath, Johan Ferret, Shreya Pathak, Nino Vieillard, Ramona Merhej, Sarah Perrin, Tatiana Matejovicova, Alexandre Ramé, Morgane Rivière, et al. Gemma 3 technical report. *arXiv preprint arXiv:2503.19786*, 2025.

[69] Omkar Thawakar, Dinura Dissanayake, Ketan More, Ritesh Thawkar, Ahmed Heakl, Noor Ahsan, Yuhao Li, Mohammed Zumri, Jean Lahoud, Rao Muhammad Anwer, Hisham Cholakkal, Ivan Laptev, Mubarak Shah, Fahad Shahbaz Khan, and Salman H. Khan. Llamav-o1: Rethinking step-by-step visual reasoning in llms. *CoRR*, abs/2501.06186, 2025. doi: 10.48550/ARXIV.2501.06186. URL <https://doi.org/10.48550/arXiv.2501.06186>.

[70] Yihe Deng, Hritik Bansal, Fan Yin, Nanyun Peng, Wei Wang, and Kai-Wei Chang. Openvlthinker: An early exploration to complex vision-language reasoning via iterative self-improvement. *CoRR*, abs/2503.17352, 2025. doi: 10.48550/ARXIV.2503.17352. URL <https://doi.org/10.48550/arXiv.2503.17352>.

[71] Yi Yang, Xiaoxuan He, Hongkun Pan, Xiyan Jiang, Yan Deng, Xingtao Yang, Haoyu Lu, Dacheng Yin, Fengyun Rao, Minfeng Zhu, Bo Zhang, and Wei Chen. R1-onevision: Advancing generalized multimodal reasoning through cross-modal formalization. *arXiv preprint arXiv:2503.10615*, 2025.

[72] Renrui Zhang, Dongzhi Jiang, Yichi Zhang, Haokun Lin, Ziyu Guo, Pengshuo Qiu, Aojun Zhou, Pan Lu, Kai-Wei Chang, Yu Qiao, et al. Mathverse: Does your multi-modal llm truly see the diagrams in visual math problems? In *European Conference on Computer Vision*, pages 169–186. Springer, 2025.

[73] Chengke Zou, Xingang Guo, Rui Yang, Junyu Zhang, Bin Hu, and Huan Zhang. Dynamath: A dynamic visual benchmark for evaluating mathematical reasoning robustness of vision language models. *arXiv preprint arXiv:2411.00836*, 2024.

[74] Pan Lu, Hritik Bansal, Tony Xia, Jiacheng Liu, Chunyuan Li, Hannaneh Hajishirzi, Hao Cheng, Kai-Wei Chang, Michel Galley, and Jianfeng Gao. Mathvista: Evaluating mathematical reasoning of foundation models in visual contexts. *arXiv preprint arXiv:2310.02255*, 2023.

[75] Runqi Qiao, Qiuna Tan, Guanting Dong, Minhui Wu, Chong Sun, Xiaoshuai Song, Zhuoma GongQue, Shanglin Lei, Zhe Wei, MiaoXuan Zhang, et al. We-math: Does your large multimodal model achieve human-like mathematical reasoning? *arXiv preprint arXiv:2407.01284*, 2024.

[76] Xiaoyi Dong, Pan Zhang, Yuhang Zang, Yuhang Cao, Bin Wang, Linke Ouyang, Xilin Wei, Songyang Zhang, Haodong Duan, Maosong Cao, et al. Internlm-xcomposer2: Mastering free-form text-image composition and comprehension in vision-language large model. *arXiv preprint arXiv:2401.16420*, 2024.

[77] Huanjin Yao, Jiaxing Huang, Wenhao Wu, Jingyi Zhang, Yibo Wang, Shunyu Liu, Yingjie Wang, Yuxin Song, Haocheng Feng, Li Shen, and Dacheng Tao. Mulberry: Empowering MLLM with o1-like reasoning and reflection via collective monte carlo tree search. *CoRR*, abs/2412.18319, 2024. doi: 10.48550/ARXIV.2412.18319. URL <https://doi.org/10.48550/arXiv.2412.18319>.

[78] Jarvis Guo, Tuney Zheng, Yuelin Bai, Bo Li, Yubo Wang, King Zhu, Yizhi Li, Graham Neubig, Wenhui Chen, and Xiang Yue. Mammoth-vl: Eliciting multimodal reasoning with instruction tuning at scale. *arXiv preprint arXiv:2412.05237*, 2024.

[79] Xuezhi Wang, Jason Wei, Dale Schuurmans, Quoc Le, Ed Chi, Sharan Narang, Aakanksha Chowdhery, and Denny Zhou. Self-consistency improves chain of thought reasoning in language models. *arXiv preprint arXiv:2203.11171*, 2022.

[80] Jiahui Gao, Renjie Pi, Jipeng Zhang, Jiacheng Ye, Wanjun Zhong, Yufei Wang, Lanqing Hong, Jianhua Han, Hang Xu, Zhenguo Li, et al. G-llava: Solving geometric problem with multi-modal large language model. *arXiv preprint arXiv:2312.11370*, 2023.

[81] Yuhao Dong, Zuyan Liu, Hai-Long Sun, Jingkang Yang, Winston Hu, Yongming Rao, and Ziwei Liu. Insight-v: Exploring long-chain visual reasoning with multimodal large language models. *arXiv preprint arXiv:2411.14432*, 2024.

[82] Yushi Hu, Weijia Shi, Xingyu Fu, Dan Roth, Mari Ostendorf, Luke Zettlemoyer, Noah A Smith, and Ranjay Krishna. Visual sketchpad: Sketching as a visual chain of thought for multimodal language models. *arXiv preprint arXiv:2406.09403*, 2024.

[83] Longhui Yu, Weisen Jiang, Han Shi, Jincheng Yu, Zhengying Liu, Yu Zhang, James T Kwok, Zhenguo Li, Adrian Weller, and Weiyang Liu. Metamath: Bootstrap your own mathematical questions for large language models. *arXiv preprint arXiv:2309.12284*, 2023.

[84] Dongyang Liu, Renrui Zhang, Longtian Qiu, Siyuan Huang, Weifeng Lin, Shitian Zhao, Shijie Geng, Ziyi Lin, Peng Jin, Kaipeng Zhang, et al. Sphinx-x: Scaling data and parameters for a family of multi-modal large language models. *arXiv preprint arXiv:2402.05935*, 2024.

[85] Zayne Sprague, Fangcong Yin, Juan Diego Rodriguez, Dongwei Jiang, Manya Wadhwa, Prasann Singhal, Xinyu Zhao, Xi Ye, Kyle Mahowald, and Greg Durrett. To cot or not to cot? chain-of-thought helps mainly on math and symbolic reasoning. *arXiv preprint arXiv:2409.12183*, 2024.

[86] Yingzhou Lu, Minjie Shen, Huazheng Wang, Xiao Wang, Capucine van Rechem, Tianfan Fu, and Wenqi Wei. Machine learning for synthetic data generation: a review. *arXiv preprint arXiv:2302.04062*, 2023.

[87] Yiming Huang, Xiao Liu, Yeyun Gong, Zhibin Gou, Yelong Shen, Nan Duan, and Weizhu Chen. Key-point-driven data synthesis with its enhancement on mathematical reasoning. *arXiv preprint arXiv:2403.02333*, 2024.

[88] Chaoyou Fu, Haojia Lin, Zuwei Long, Yunhang Shen, Meng Zhao, Yifan Zhang, Shaoqi Dong, Xiong Wang, Di Yin, Long Ma, et al. Vita: Towards open-source interactive omni multimodal llm. *arXiv preprint arXiv:2408.05211*, 2024.

[89] Zhibin Gou, Zhihong Shao, Yeyun Gong, Yelong Shen, Yujiu Yang, Nan Duan, and Weizhu Chen. Critic: Large language models can self-correct with tool-interactive critiquing. *arXiv preprint arXiv:2305.11738*, 2023.

[90] Bofei Gao, Zefan Cai, Runxin Xu, Peiyi Wang, Ce Zheng, Runji Lin, Keming Lu, Junyang Lin, Chang Zhou, Wen Xiao, et al. Llm critics help catch bugs in mathematics: Towards a better mathematical verifier with natural language feedback. *CoRR*, 2024.

[91] Zicheng Lin, Zhibin Gou, Tian Liang, Ruilin Luo, Haowei Liu, and Yujiu Yang. CriticBench: Benchmarking LLMs for critique-correct reasoning. In Lun-Wei Ku, Andre Martins, and Vivek Srikumar, editors, *Findings of the Association for Computational Linguistics: ACL 2024*, pages 1552–1587, Bangkok, Thailand, August 2024. Association for Computational Linguistics. doi: 10.18653/v1/2024.findings-acl.91. URL <https://aclanthology.org/2024.findings-acl.91>.

[92] Aviral Kumar, Vincent Zhuang, Rishabh Agarwal, Yi Su, John D Co-Reyes, Avi Singh, Kate Baumli, Shariq Iqbal, Colton Bishop, Rebecca Roelofs, et al. Training language models to self-correct via reinforcement learning. *arXiv preprint arXiv:2409.12917*, 2024.

[93] Charlie Snell, Jaehoon Lee, Kelvin Xu, and Aviral Kumar. Scaling llm test-time compute optimally can be more effective than scaling model parameters. *arXiv preprint arXiv:2408.03314*, 2024.

[94] Haoqin Tu, Weitao Feng, Hardy Chen, Hui Liu, Xianfeng Tang, and Cihang Xie. Vilbench: A suite for vision-language process reward modeling. *arXiv preprint arXiv:2503.20271*, 2025.

[95] Weiyun Wang, Zhangwei Gao, Lianjie Chen, Zhe Chen, Jinguo Zhu, Xiangyu Zhao, Yangzhou Liu, Yue Cao, Shenglong Ye, Xizhou Zhu, et al. Visualprm: An effective process reward model for multimodal reasoning. *arXiv preprint arXiv:2503.10291*, 2025.

[96] Linzhuang Sun, Hao Liang, Jingxuan Wei, Bihui Yu, Tianpeng Li, Fan Yang, Zenan Zhou, and Wentao Zhang. Mm-verify: Enhancing multimodal reasoning with chain-of-thought verification. *arXiv preprint arXiv:2502.13383*, 2025.

[97] Bofei Gao, Zefan Cai, Runxin Xu, Peiyi Wang, Ce Zheng, Runji Lin, Keming Lu, Junyang Lin, Chang Zhou, Wen Xiao, Junjie Hu, Tianyu Liu, and Baobao Chang. LLM critics help catch bugs in mathematics: Towards a better mathematical verifier with natural language feedback. *CoRR*, abs/2406.14024, 2024. doi: 10.48550/ARXIV.2406.14024. URL <https://doi.org/10.48550/arXiv.2406.14024>.

[98] Weihao Zeng, Yuzhen Huang, Lulu Zhao, Yijun Wang, Zifei Shan, and Junxian He. B-star: Monitoring and balancing exploration and exploitation in self-taught reasoners. *arXiv preprint arXiv:2412.17256*, 2024.

[99] Fanqing Meng, Lingxiao Du, Zongkai Liu, Zhixiang Zhou, Quanfeng Lu, Daocheng Fu, Botian Shi, Wenhui Wang, Junjun He, Kaipeng Zhang, et al. Mm-eureka: Exploring visual aha moment with rule-based large-scale reinforcement learning. *arXiv preprint arXiv:2503.07365*, 2025.

[100] Leandro von Werra, Younes Belkada, Lewis Tunstall, Edward Beeching, Tristan Thrush, Nathan Lambert, Shengyi Huang, Kashif Rasul, and Quentin Gallouédec. Trl: Transformer reinforcement learning. <https://github.com/huggingface/trl>, 2020.

[101] Jinze Bai, Shuai Bai, Shusheng Yang, Shijie Wang, Sinan Tan, Peng Wang, Junyang Lin, Chang Zhou, and Jingren Zhou. Qwen-vl: A versatile vision-language model for understanding, localization, text reading, and beyond. *arXiv preprint arXiv:2308.12966*, 1(2):3, 2023.

[102] Hugging Face. Open r1: A fully open reproduction of deepseek-r1, January 2025. URL <https://github.com/huggingface/open-r1>.

[103] P Kingma Diederik. Adam: A method for stochastic optimization. (*No Title*), 2014.

[104] Yanli Zhao, Andrew Gu, Rohan Varma, Liang Luo, Chien-Chin Huang, Min Xu, Less Wright, Hamid Shojanazeri, Myle Ott, Sam Shleifer, Alban Desmaison, Can Balioglu, Pritam Damania, Bernard Nguyen, Geeta Chauhan, Yuchen Hao, Ajit Mathews, and Shen Li. Pytorch FSDP: experiences on scaling fully sharded data parallel. *Proc. VLDB Endow.*, 16(12):3848–3860, 2023. doi: 10.14778/3611540.3611569. URL <https://www.vldb.org/pvldb/vol16/p3848-huang.pdf>.

[105] Woosuk Kwon, Zhuohan Li, Siyuan Zhuang, Ying Sheng, Lianmin Zheng, Cody Hao Yu, Joseph Gonzalez, Hao Zhang, and Ion Stoica. Efficient memory management for large language model serving with pagedattention. In *Proceedings of the 29th Symposium on Operating Systems Principles*, pages 611–626, 2023.

[106] Jingcheng Hu, Yinmin Zhang, Qi Han, Dixin Jiang, Xiangyu Zhang, and Heung-Yeung Shum. Open-reasoner-zero: An open source approach to scaling up reinforcement learning on the base model. *CoRR*, abs/2503.24290, 2025. doi: 10.48550/ARXIV.2503.24290. URL <https://doi.org/10.48550/arXiv.2503.24290>.

[107] Ke Wang, Junting Pan, Weikang Shi, Zimu Lu, Mingjie Zhan, and Hongsheng Li. Measuring multimodal mathematical reasoning with math-vision dataset. *arXiv preprint arXiv:2402.14804*, 2024.

Appendices Content

A	Related Work	18
B	Preliminary	18
	B.1 Group Relative Policy Optimization	18
	B.2 Test-Time Scaling by Best-of-N evaluation	19
C	Supplementary Results	19
	C.1 Fine-grained Comparison on Used benchmarks	19
	C.2 Scaling Law of MMathCoT-1M	20
	C.3 Higher Upper Bound Taken from Stage I	21
	C.4 Generalization Validation	21
	C.5 Implementary Results on Other Benchmarks	22
D	Module Selection Criteria	22
E	Ablation Studies	23
	E.1 Effectiveness of Different Data Category	23
	E.2 Selection of External Closed-source MLLM	24
F	Implementation Details	25
	F.1 RL Data Curation	25
	F.2 Parameters and Time Cost	25
	F.3 Benchmarks	25
	F.4 Algorithm	26
G	Prompt Design	28
	G.1 Prompt Utilized in MMathCoT-1M Synthesis	28
	G.2 Prompt Utilized in DualMath-1.1M Synthesis	29
H	Case Study	30
	H.1 Showcase on Best-of-N Evaluation	30
	H.2 Process of Misinterpretation Insertion Engine	30
	H.3 Failure Pattern in Process During GRPO	30
	H.4 Cases on How Naive Process Reward Modeling Fails	31

A Related Work

Multimodal Math Reasoning The mathematical reasoning capabilities of MLLMs have recently attracted significant attention [11, 80, 35, 81, 82, 5, 14, 78]. Unlike traditional mathematical reasoning tasks in Language Models (LLMs) [1, 83], multimodal mathematical reasoning requires MLLMs to interpret visual information and perform cross-modal reasoning between images and text. Tasks such as solving geometric problems and analyzing graphs are particularly challenging [40]. Recent advances have focused on improving visual mathematical input specialized encoders in specific scenarios [19, 84, 61]. A significant emphasis has also been placed on synthesizing diverse and complex training data. For instance, Math-LLaVA [15] introduces the MathV360K dataset, which categorizes images by complexity and enhances associated questions. Multimath [23] curates high-quality reasoning data from K-12 textbooks and employs GPT-4 for CoT data generation and validation. R-CoT [17] further diversifies problems through a two-stage reverse question-answer generation process. These data synthesis methods are widely adopted in academia and industry due to their demonstrated efficiency [85–88].

Process Reward Model Recent studies have explored test-time scaling laws in LLMs, aiming to identify optimal reasoning trajectories from diverse thinking trajectories [26, 89–91, 31, 92, 93]. Initial efforts, such as self-consistency [79], have laid the groundwork for test-time scaling. OpenAI has introduced verifiers to supervise and select reasoning paths during inference [41]. Math-Shepherd [43] evaluates intermediate reasoning steps based on their likelihood of leading to correct answers, while OmegaPRM [42] constructs PRM training data and employs MCTS for training. Despite these advancements, the lack of models with robust CoT reasoning capabilities and limited exploration into diverse reward model training data remain significant bottlenecks in multimodal mathematical reasoning. Some concurrent work also begins to pay attention to PRM-assisted visual reasoning, such as construction and benchmarking [94–96].

B Preliminary

B.1 Group Relative Policy Optimization

Vanilla GRPO eliminates value function in PPO and estimates the advantages within online rollout group. Given a question with image q and ground-truth y , policy model $\pi_{\theta_{old}}$ samples a group of G responses $\{o^i\}_{i=1}^G$. GRPO compute the i -th response's advantage through normalizing in-group rewards $\{r^j\}_{j=1}^G$, and employs PPO's clipped objective and KL penalty term:

$$A^i = \frac{r^i - \text{mean}(\{r^j\}_{j=1}^G)}{\text{std}(\{r^j\}_{j=1}^G)} \quad (7)$$

$$\begin{aligned} \mathcal{J}_{GRPO}(\theta) = & \mathbb{E}_{(q,y) \sim \mathcal{D}, \{o^i\}_{i=1}^G \sim \pi_{\theta_{old}}(\cdot|q)} \\ & \left[\frac{1}{G} \sum_{i=1}^G \frac{1}{|o^i|} \sum_{t=1}^{|o^i|} (\min(r_t^i(\theta)A^i, \text{clip}(r_t^i(\theta), 1-\epsilon, 1+\epsilon)A^i) - \beta D_{KL}^{i,t}(\pi_\theta || \pi_{ref})) \right] \end{aligned} \quad (8)$$

We introduce the two variants of PRM-integrated GRPO discussed in Section 4. Given PRM \mathcal{M}_p and process reward sequences $r_s = \mathcal{M}_p(\{s_1, s_2, \dots, s_N\})$ (i) *Variant 1*: Given verifiable outcome reward r_o^i , we set a single rollout's reward as $r^i = r_o^i + r_s^i$. (ii) *Variant 2*: We utilize a step-level reward and a multiple relative advantage calculated by the mean value of process rewards from each rollout:

$$A_t^i = r_{s,t}^i \underbrace{\frac{\bar{r}_s^i - \text{mean}(\{\bar{r}_s^j\}_{j=1}^G)}{\text{std}(\{\bar{r}_s^j\}_{j=1}^G)}}_{\text{GRPO with process rewards}} + \underbrace{\frac{r_o^i - \text{mean}(\{r_o^j\}_{j=1}^G)}{\text{std}(\{r_o^j\}_{j=1}^G)}}_{\text{GRPO with outcome rewards}} \quad (9)$$

in which $\bar{r}_s^i = \text{mean}(\mathcal{M}_p(\{s_1^i, s_2^i, \dots, s_{T_i}^i\}))$.

B.2 Test-Time Scaling by Best-of-N evaluation

Following previous works [41, 43], we adopt BoN evaluation for TTS. Given N response samplings for a question q . The PRM is used to give process reward for each sampling. We use mean value of process rewards to select the best single sampling:

$$a_{\text{prm}} = \arg \max_{s_i} \text{mean}\{\mathcal{M}_p(q, s_i)\} \quad (10)$$

Some other works [97] merge self-consistency and PRM to employ a voting-based score cumulation. But we don't select this method for a simpler evaluation manner.

C Supplementary Results

C.1 Fine-grained Comparison on Used benchmarks

In this section, we provide some fine-grained results for a clearer comparison. As demonstrated in Table 5, our proposed methods demonstrate significant advantages. Compared to closed-source models like GPT-4o and GPT-4V, our URSA-8B and URSA-8B-PS-GRPO show strong competitiveness. Among open-source models, the performance improvements are even more evident. Our URSA-8B model outperforms other open-source models such as InternLM-XComposer2-VL and Ovis1.6-Gemma2-9B in most subtasks. When combined with PS-GRPO, the URSA-8B-PS-GRPO model achieves even better results, showing significant improvements in subtasks like Alg, AnaG, CombG, and others. Our methods particularly excel in complex mathematical reasoning tasks, demonstrating their powerful mathematical reasoning capabilities. These results highlight the effectiveness of our proposed MMathCoT-1M and PS-GRPO methods in enhancing the mathematical reasoning abilities of models, especially in visual mathematical problems.

In Dynamath (Table 6), compared to open-source MLLMs, the URSA series has obvious advantages in plane geometry and algebra. Surprisingly, from the knowledge level classification, the URSA series model performs excellently at the undergraduate level, which is partly attributable to its math-intensive alignment and large-scale instruction fine-tuning.

In MathVerse (Table 7), we can see that URSA series model marginally surpass GPT-4o on average. Besides, compared with other open-source MLLMs, URSA-8B-PS-GRPO outperforms leading AtomThink-EMOVA-8B and InternVL2.5-8B with **8.4** and **11.4** points. In WE-MATH 8, URSA-

Table 5: Performance comparison of different MLLMs on MathVision.

Model	Size	ALL	Alg	AnaG	Ari	CombG	Comb	Cnt	DescG	GrphT	Log	Angle	Area	Len	SoIG	Stat	Topo	TransG
<i>Baselines</i>																		
Human	-	68.8	55.1	78.6	99.6	98.4	43.5	98.5	91.3	62.2	61.3	33.5	47.2	73.5	87.3	93.1	99.8	69.0
<i>Closed-source MLLMs</i>																		
GPT-4o	-	30.4	42.0	39.3	49.3	28.9	25.6	22.4	24.0	23.3	29.4	17.3	29.8	30.1	29.1	44.8	34.8	17.9
GPT-4V	-	22.8	27.3	32.1	35.7	21.1	16.7	13.4	22.1	14.4	16.8	22.0	22.2	20.9	23.8	24.1	21.7	25.6
CoT GPT-4V	-	24.0	26.7	26.2	38.6	22.1	24.4	19.4	27.9	23.3	25.2	17.3	21.4	23.4	23.8	25.9	4.4	25.6
Gemini-1.5-Pro	-	19.2	20.3	35.7	34.3	19.8	20.9	26.0	26.7	22.7	14.5	14.4	16.5	18.9	10.3	26.1	17.3	
<i>Open-source MLLMs</i>																		
LLaVA-1.5	7B	8.5	7.0	7.1	10.7	7.1	4.8	10.5	7.7	10.0	9.2	15.6	10.2	9.8	5.3	8.6	4.4	4.8
LLaVA-1.5	13B	11.1	7.0	14.3	14.3	9.1	6.6	6.0	13.5	5.6	13.5	10.4	12.6	14.7	11.5	13.8	13.0	10.7
InternLM-XComposer2-VL	7B	14.5	9.3	15.5	12.1	15.3	11.3	10.5	14.4	22.2	19.3	19.7	15.6	15.0	11.9	15.5	26.1	15.5
Ovis1.6-Gemma2-9B	9B	18.8	13.3	15.5	22.1	17.9	11.3	22.4	23.1	20.0	20.2	20.8	18.0	24.7	15.6	20.7	17.4	20.8
MinICPM-v2.6	8B	18.4	9.9	19.0	18.6	21.8	13.1	13.4	17.3	20.0	16.0	25.4	19.4	20.7	15.2	27.6	30.4	22.0
LLaVA-OneVision	8B	18.3	11.6	16.7	20.7	18.5	11.9	14.9	19.2	13.3	20.2	17.9	21.6	23.4	12.3	22.4	13.0	24.4
Qwen2-VL	8B	19.2	15.4	20.2	19.3	16.9	16.7	17.9	22.1	22.2	16.0	19.1	22.4	22.5	14.8	19.0	4.3	23.8
InternVL2-8B	8B	18.4	18.6	22.6	28.6	22.1	13.7	10.4	11.5	13.3	21.0	20.8	22.4	20.5	16.8	17.2	26.1	24.2
InternVL2.5-8B	8B	19.7	15.1	23.8	29.3	16.2	8.9	11.9	10.6	8.9	18.5	22.0	19.4	15.4	13.9	22.4	21.7	19.6
<i>Open-source Math MLLMs</i>																		
Math-LLaVA	13B	15.7	9.0	20.2	15.7	18.2	10.1	10.5	16.4	14.4	16.0	20.2	18.4	17.6	9.4	24.1	21.7	17.9
Multimath	7B	16.3	11.3	21.1	15.5	15.9	11.3	12.1	15.5	15.9	18.5	20.1	16.4	21.3	13.3	14.6	13.3	20.8
Math-PUMA-Qwen2-7B	8B	14.0	5.9	21.1	21.1	21.1	11.0	5.6	15.7	10.5	13.8	11.7	15.8	12.2	17.8	19.2	15.8	12.2
MAVIS	7B	18.5	17.5	19.5	21.5	19.0	12.0	14.0	18.0	16.0	19.0	21.0	18.5	19.5	15.0	19.0	20.0	20.0
AtomThink-EMOVA	8B	24.9	23.5	25.5	32.0	21.0	15.8	19.5	21.5	22.5	21.5	26.5	25.5	26.5	27.5	28.0	23.0	22.5
URSA-8B	8B	28.7	28.1	26.2	35.0	22.1	15.5	19.4	18.3	22.2	21.8	37.0	27.0	26.5	31.1	27.6	17.4	23.8
URSA-8B-PS-GRPO	8B	31.5	30.1	28.6	29.3	31.5	20.8	20.9	26.9	17.8	24.4	35.8	33.6	37.2	37.7	25.9	26.1	35.1

series outperforms leading general-purpose and math reasoning MLLMs in three-stage accuracy. Also, the URSA series has remarkable strengths in solid figures, transformations, positions, and directions. This is mainly due to large-scale alignment and instruction tuning, which builds its foundation in understanding mathematical elements.

Table 6: Detailed performance comparison of MLLMs on **DYNAMATH** *testmini* dataset, broken down by subject area and knowledge level.

Model	Size	ALL	PG	SG	AG	AL	PT	GT	AR	Elem.	High	Undergrad.
<i>Closed-source MLLMs</i>												
GPT-4o	-	64.9	56.8	52.0	61.0	76.9	51.8	58.1	61.5	68.6	61.8	36.8
Claude-3.5-Sonnet	-	64.8	49.9	49.3	55.3	81.0	44.1	69.4	61.2	66.7	62.6	33.3
Gemini-1.5-Pro	-	60.5	52.7	42.7	61.6	70.8	20.6	65.2	54.2	62.9	59.2	37.1
<i>Open-source MLLMs</i>												
Llava-v1.5-7B	7B	16.6	10.5	7.3	19.5	6.5	8.2	32.3	10.8	18.9	13.3	11.7
Llava-v1.6-34B	34B	27.1	21.4	25.3	27.6	14.9	7.6	32.7	23.1	35.9	23.8	16.6
Deepseek-VL-7B-Chat	7B	21.5	16.0	13.3	26.5	12.9	4.7	32.3	12.7	28.3	19.0	16.0
InternVL2-8B	8B	39.7	33.9	37.3	32.5	46.9	15.9	42.1	37.3	51.1	37.4	19.6
Qwen2-VL	8B	42.1	40.3	38.7	39.9	37.1	8.2	44.8	39.2	47.6	42.2	24.4
AtomThink-EMOVA	8B	40.9	42.0	37.9	33.6	58.0	23.0	44.0	38.4	52.5	43.5	32.0
URSA-8B	8B	44.7	48.1	38.0	33.7	66.9	24.7	39.2	38.5	53.5	44.3	41.8
URSA-8B-PS-GRPO	8B	47.4	49.7	40.1	35.2	65.7	24.7	45.2	41.1	53.5	46.7	43.2

Table 7: Comparison with closed-source MLLMs and open-source MLLMs on **MATHVERSE** *testmini*. The best results of Closed-source MLLMs are highlighted. The best and second-best results of Open-source MLLMs are highlighted.

Model	#Params	ALL	TD	TL	TO	VI	VD	VO
<i>Baselines</i>								
Random	-	12.4	12.4	12.4	12.4	12.4	12.4	12.4
Human	-	64.9	71.2	70.9	41.7	61.4	68.3	66.7
<i>Closed-Source MLLMs</i>								
GPT-4o	-	50.8	59.8	50.3	52.4	48.0	46.5	47.6
GPT-4V	-	39.4	54.7	41.4	48.7	34.9	34.4	31.6
Gemini-1.5-Flash-002	-	49.4	57.2	50.5	50.3	47.6	45.1	45.4
Gemini-1.5-Pro	-	35.3	39.8	34.7	44.5	32.0	36.8	33.3
Claude-3.5-Sonnet	-	-	-	-	-	-	-	-
Qwen-VL-Plus	-	21.3	26.0	21.2	25.2	18.5	19.1	21.8
<i>Open-Source General MLLMs</i>								
mPLUG-Owl2-7B	7B	10.3	11.6	11.4	13.8	11.1	9.4	8.0
MiniGPT4-7B	7B	12.2	12.3	12.9	13.4	12.5	14.8	8.7
LLaVA-1.5-13B	13B	12.7	17.1	12.0	22.6	12.6	12.7	9.0
SPHINX-V2-13B	13B	16.1	20.8	14.1	14.0	16.4	15.6	16.2
LLaVA-NeXT-34B	34B	34.6	49.0	37.6	30.1	35.2	28.9	22.4
InternLM-XComposer2-VL	7B	25.9	36.9	28.3	42.5	20.1	24.4	19.8
Deepseek-VL	8B	19.3	23.0	23.2	23.1	20.2	18.4	11.8
LLaVA-OneVision (SI)	8B	28.9	29.0	31.5	34.5	30.1	29.5	26.9
Qwen2-VL	8B	33.6	37.4	33.5	35.0	31.3	30.3	28.1
InternVL2-8B	8B	35.9	39.0	33.8	36.0	32.2	30.9	27.7
InternVL2.5-8B	8B	39.5	43.0	43.0	43.0	42.2	42.2	22.8
<i>Open-Source Math MLLMs</i>								
G-LLaVA-7B	7B	16.6	20.9	20.7	21.1	17.2	14.6	9.4
Math-LLaVA-13B	13B	22.9	27.3	24.9	27.0	24.5	21.7	16.1
Math-PUMA-Qwen2-7B	8B	33.6	42.1	35.0	39.8	33.4	31.6	26.0
Math-PUMA-DeepSeek-Math	7B	31.8	43.4	35.4	47.5	33.6	31.6	14.7
MAVIS-7B	7B	35.2	43.2	37.2	35.2	34.1	29.7	31.8
InfinMM-Math	7B	40.5	46.7	39.4	41.6	38.1	40.4	27.8
Multimath-7B	7B	27.7	34.8	30.8	35.3	28.1	25.9	15.0
AtomThink-EMOVA	8B	42.5	48.1	47.7	45.7	44.0	44.2	26.8
URSA-8B	8B	45.7	55.3	48.3	51.8	46.4	43.9	28.6
URSA-8B-PS-GRPO	8B	50.9	57.3	52.2	50.2	48.7	47.6	31.5

C.2 Scaling Law of MMathCoT-1M

To better illustrate the effectiveness of MMathCoT-1M, we examine the scaling laws of SFT by training models on randomly selected samples representing various ratios of the full dataset.

As shown in Table 9, we can see that MMathCoT-1M clearly shows a training time scaling law, further validates the effectiveness of the synthesized data.

Table 8: Accuracy comparison with closed-source MLLMs and open-source MLLMs on **WE-MATH testmini** subset. First 3 columns show the overall performance on one-step, two-step and three-step problems. The other columns are used to demonstrate the performance in different problem strategies. Red indicates the best performance and Blue indicates the second best performance among open-source models.

Model	#Params	S1	S2	S3	Mem			PF			SF			TMF			PD		
		UCU	AL	CPF	UPF	CSF	USF	BTF	CCF	Dir	Pos	RoM	CCP	Dir	Pos	RoM	CCP		
<i>Closed-source MLLMs</i>																			
GPT-4o	-	72.8	58.1	43.6	86.6	39.1	77.4	71.6	84.5	62.3	58.7	69.4	93.1	72.7	47.5	73.3			
GPT-4V	-	65.5	49.2	38.2	82.5	38.4	70.7	60.2	76.6	56.3	57.8	67.7	79.3	57.5	47.8	63.3			
Gemini-1.5-Pro	-	56.1	51.4	33.9	51.0	31.2	61.8	45.0	70.0	57.5	39.2	62.7	68.8	54.1	40.7	60.0			
Qwen-VL-Max	-	40.8	30.3	20.6	19.4	25.3	39.8	41.4	43.6	48.0	43.8	43.4	41.4	35.1	40.7	26.7			
<i>Open-source General MLLMs</i>																			
LLaVA-1.6	7B	23.0	20.8	15.8	18.5	20.5	16.9	29.6	15.6	18.6	42.7	24.1	17.6	43.3	28.9	26.7			
LLaVA-1.6	13B	29.4	25.3	32.7	21.7	23.2	23.4	34.7	25.3	26.4	37.5	41.7	26.9	28.9	37.1	30.0			
GLM-4V-9B	9B	47.3	37.2	38.2	53.4	37.0	51.3	46.5	50.6	38.2	44.1	45.2	41.0	49.3	36.8	53.3			
MiniCPM-LLaMA3-V2.5	8B	39.8	31.1	29.7	28.6	37.0	40.8	39.8	41.0	38.6	32.0	42.7	41.0	42.7	44.0	43.3			
LongVA	7B	43.5	30.6	28.5	24.5	39.8	45.1	40.8	51.9	42.5	45.6	44.6	44.5	40.7	47.5	20.0			
InternLM-XComposer2-VL	7B	47.0	33.1	33.3	31.3	46.5	47.7	42.6	51.4	43.9	41.1	50.6	65.5	53.9	55.2	40.0			
Phi3-Vision	4.2B	42.1	34.2	27.9	28.7	16.0	47.2	38.8	50.0	44.4	28.8	31.2	48.6	49.2	26.4	50.0			
DeepSeek-VL	7B	32.6	26.7	25.5	16.6	35.1	27.3	38.0	24.2	38.7	50.0	23.3	24.5	41.0	51.7	23.3			
InternVL2-8B	8B	59.4	43.6	35.2	71.4	20.5	62.0	55.5	67.1	57.3	54.0	60.5	58.6	63.6	44.5	50.0			
InternVL2.5-8B	8B	58.7	43.1	38.8	48.7	35.8	65.5	54.5	62.3	61.5	47.8	60.3	79.0	64.0	51.1	63.3			
Qwen2-VL	8B	59.1	43.6	26.7	62.7	37.2	62.6	60.8	65.7	49.2	52.5	49.2	48.1	68.2	55.0	56.7			
Gemma3-12B	12B	64.3	47.2	42.1	83.1	33.9	70.2	58.2	77.5	61.1	50.1	63.7	82.6	58.4	36.8	60.0			
<i>Open-source Math MLLMs</i>																			
G-LLaVA	7B	32.4	30.6	32.7	33.3	29.1	32.0	37.9	19.6	33.5	37.1	32.8	31.2	33.2	25.6	40.0			
Math-LLaVA	13B	38.7	34.2	34.6	30.3	17.9	39.2	40.4	37.1	37.7	53.0	51.3	30.8	30.8	40.9	46.7			
Math-PUMA-Qwen2-7B	8B	53.3	39.4	36.4	63.5	42.5	60.2	45.9	66.2	48.6	42.3	53.5	31.2	37.7	40.4	46.7			
MAVIS w/o DPO	7B	56.9	37.1	33.2	-	-	-	-	-	-	-	-	-	-	-	-			
MAVIS	7B	57.2	37.9	34.6	-	-	-	-	-	-	-	-	-	-	-	-			
URSA-8B	8B	63.1	56.4	41.8	59.1	32.5	72.3	60.3	70.9	66.0	51.4	59.8	58.3	39.5	58.8	53.3			
URSA-8B-PS-GRPO	8B	68.6	64.2	52.7	52.6	63.5	68.5	64.1	68.8	73.6	69.4	75.8	72.1	72.6	73.6	63.3			

Table 9: Scaling law validation on URSA-8B using different ratios of the MMathCoT-1M.

Ratio	MathVerse	MathVision	MathVista-GPS	WEMATH	DYNAMATH
1/4	34.7	20.5	68.5	43.5	36.6
1/2	40.5	22.8	72.3	47.7	38.8
3/4	42.0	26.7	77.9	50.9	42.2
1	45.7	28.7	81.7	53.6	44.7

C.3 Higher Upper Bound Taken from Stage I

In Stage I, we obtain a more powerful base MLLM with enhanced reasoning capabilities through math-intensive vision-language alignment and instruction fine-tuning. Beyond the results in Table 1, we explain why Stage I can better serve subsequent experiments, focusing on test-time scaling and PRM applications. We select MathVerse, MathVision, and MathVista-GPS to observe the **pass@N** metric. As demonstrated in Figure 7, we find that URSA-8B consistently outperforms current leading general MLLMs and math reasoning MLLMs. This indicates that while current trends favor RL-related techniques, the scaling law of supervised fine-tuning can still demonstrate its role in breaking through the base model’s limitations. This naturally brings advantages in areas such as BoN evaluation and the proportion of valuable rollouts in online RL. First, URSA-8B’s higher upper bound leads to richer and more reliable process label generation in Stage II. Furthermore, since recent works claims that RL can only approach the optimal solution within its own exploration path [29, 4, 98], Stage I naturally expands the potential upper limit of the RL stage. This provides the most fundamental advantage to the performance of URSA-PS-GRPO-8B.

C.4 Generalization Validation

To further validate the effectiveness of proposed MMathCoT-1M and PRM aided PS-GRPO. We select InternVL2.5-8B from the general-purpose MLLMs and Multimath from the math reasoning MLLMs for a generalization validation experiment. We do not conduct additional hyperparameter tuning but almost directly adopt the settings from Table 13. The experiment on InternVL2.5-8B and Multimath are implemented on Meng et al. [99] and TRL [100]. Given that these two models

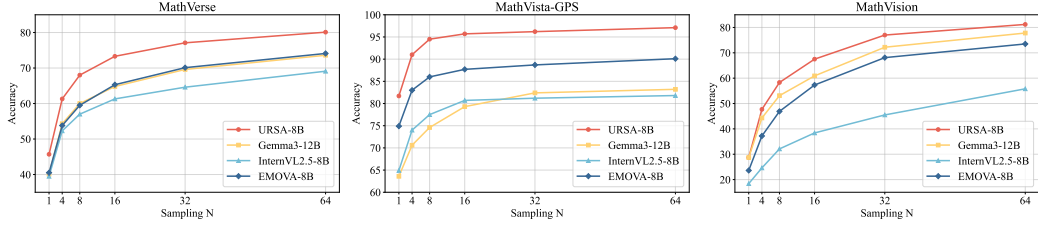


Figure 7: Pass@N evaluation on three benchmarks.

Figure 8: The progress of MMathCoT-1.1M and URSA-8B-RM aided PS-GRPO on InternVL2.5-8B and MultiMath.

Model	Avg	MathVerse testmini	MathVision full set	MathVista gps	WE-MATH testmini	DYNAMATH testmini	GeoQA full set
InternVL2.5-8B	45.2	39.5	19.7	64.9	44.7	40.5	61.6
+ MMathCoT-1.1M	51.7 (↑6.5)	43.3 (↑3.8)	25.9 (↑6.2)	77.9 (↑13.0)	49.1 (↑4.4)	45.3 (↑4.8)	68.8 (↑7.2)
+ PS-GRPO	54.7 (↑9.5)	47.5 (↑8.0)	28.5 (↑8.8)	80.1 (↑15.2)	55.3 (↑10.6)	45.9 (↑5.4)	71.1 (↑9.5)
MultiMath	43.1	27.7	16.3	66.8	42.2	37.9	67.7
+ MMathCoT-1.1M	48.7 (↑5.6)	36.9 (↑9.2)	22.7 (↑6.4)	74.4 (↑7.6)	45.8 (↑3.6)	40.4 (↑2.5)	72.2 (↑4.5)
+ PS-GRPO	51.2 (↑8.1)	39.7 (↑12.0)	24.4 (↑8.1)	77.7 (↑10.9)	49.3 (↑7.1)	42.6 (↑4.7)	73.5 (↑5.8)

Table 10: Comparison of TTS with different models using BoN performance on WE-MATH, DYNAMATH, and GeoQA.

Model	Method	WE-MATH				DYNAMATH				GeoQA			
		N=4	N=8	N=16	N=32	N=4	N=8	N=16	N=32	N=4	N=8	N=16	N=32
URSA-8B	Self-Consistency	56.3	57.0	57.7	58.0	46.2	46.7	47.5	48.0	74.1	75.3	75.9	75.9
	InternVL2.5-8B ORM	56.0	56.8	57.4	57.7	45.9	46.5	47.2	47.7	73.8	75.0	75.6	75.6
	URSA-8B-RM	58.2	59.0	59.3	59.7	47.5	48.4	49.5	50.5	76.1	77.3	78.0	78.1
AtomThink-EMOVA	Self-Consistency	51.7	52.4	52.9	53.6	42.3	43.0	43.7	44.0	65.7	66.5	66.6	66.8
	InternVL2.5-8B ORM	51.5	52.2	52.7	53.3	42.1	42.8	43.5	43.7	65.5	66.3	66.4	66.6
	URSA-8B-RM	53.7	54.5	55.0	55.8	44.1	44.9	45.6	46.0	67.9	68.8	69.0	69.3

have already undergone sufficient alignment for general domains or specific vertical domains upon their release, we only carry out two stages of training: (i) MMathCoT-1M is used to enhance the base model’s mathematical reasoning capabilities; (ii) URSA-8B-RM is involved in the PS-GRPO process. We present the results in Table 8. The proposed MMathCoT-1M and PRM aided PS-GRPO demonstrate remarkable generalization capabilities across different models and benchmarks. When applied to InternVL2.5-8B and MultiMath, both models show significant performance improvements. For InternVL2.5-8B, adding MMathCoT-1M boosts the average score from 45.2 to 51.7, with even more significant gains when combined with PS-GRPO, reaching 54.7. Similarly, for MultiMath, the average score increases from 43.1 to 48.7 with MMathCoT-1M and further to 51.2 with PS-GRPO. These results highlight the effectiveness of our approach in enhancing mathematical reasoning capabilities across diverse models and tasks. The performance improvements are consistent across various benchmarks, including MathVerse, MathVision, MathVista, WE-MATH, DYNAMATH, and GeoQA, indicating that our methods are not only effective but also broadly applicable.

C.5 Implementary Results on Other Benchmarks

We provide supplementary results on WE-MATH, DYNAMATH and GeoQA when comparing BoN selection. As shown in table 10, URSA-8B-RM remains an advantage with Self-consistency and InternVL2.5-8B ORM. When employing URSA-8B as reasoning model, URSA-8B-RM outperforms Self-consistency with 4.6%, 4.5% and 2.7% relative improvements in Best-of-8 performance.

D Module Selection Criteria

As for module selection, we primarily considered the choice of the vision encoder and the LLM backbone.

Vision Encoder To train a reasoning model with higher process sensibility and facilitate PRM training, we first conduct captioning tests on open-source models like DeepSeek-VL, Qwen2-VL, etc., using a manually selected dataset (approximately 80 examples). These examples primarily include function-related and geometry problems prone to visual confusion. We manually inspect the outputs of these open-source models and find that Qwen2-VL and LLaVA-OneVision performed poorly; even though their performance on standard benchmarks is good, they fail to ensure sufficiently accurate mathematical descriptions. However, DeepSeekVL’s native hybrid vision tower design, integrating high- and low-resolution processing, subjectively exhibit better recognition accuracy. We speculate that this is due to QwenViT [101] being more heavily biased towards general multimodal tasks, resulting in less precise mathematical descriptions compared to simpler vision backbones. Therefore, we choose the SigLiP-L+SAM-B hybrid vision tower design.

LLM Backbone Considering the open-source influence of the QwenLM-Series, we follow the choice of prior work such as MathPUMA [11] and Multimath [23] by using the QwenLM-Series backbone. However, we consider whether we could achieve higher performance by leveraging instruction models that has undergone unimodal math post-training, and thus compare Qwen2.5-7B-Instruct¹ and Qwen2.5-Math-7B-Instruct². After completing the VL alignment stage, we conduct a small-scale comparative experiment on MMathCoT-1M, fine-tuning on 50K examples. Finally, our results show that using Qwen2.5-Math-Instruct as the backbone yields an advantage of approximately 1 percentage point on MathVision and MathVerse. Therefore, we include Qwen2.5-Math-7B-Instruct as the LLM backbone for subsequent experiments.

E Ablation Studies

E.1 Effectiveness of Different Data Category

In the first stage, we mainly synthesized large-scale multiclass CoT data.

- **w/o S_{A_0} :** In this variant, the answer-only data is reverted to its original format. This directly mimics the training mode used by models such as Math-LLaVA and Math-PUMA, which involves hybrid training on both direct answers ('fast thinking') and CoT thinking.
- **w/o S_{A_n} :** This data will be replaced with its original organizational structure, where the analysis and final answer are provided in a free-form text format.
- **w/o S_C :** This batch of data will be replaced with reasoning expressed in mathematical formal language, better reflecting symbolic and 'plan and reasoning' forms of reasoning.

The results are shown in Figure 9. Firstly, it is shown across all datasets that using the complete synthesized data achieves the best results, highlighting the role of MMathCoT-1M data. More specifically, we find: i) S_{A_0} demonstrates the greatest impact on MathVerse and MathVision, indicating that expanded CoT data is important for problems where absolute solution accuracy is pursued; ii) However, on WE-MATH, the replacement of S_{A_n} leads to the most significant performance drop, suggesting that content rewriting better aligns with the end-to-end requirements posed by the WE-MATH benchmark, and mixing training with data lacking clear logical sequences may reduce hierarchical accuracy; iii) The results on DYNAMATH indicate that rewriting and natural language formulation effectively enhance reasoning robustness from the perspective of textual diversity. This reveals that the thought pattern in textual form tends to maintain the stability of the thought process more effectively under scenarios involving image transformations.

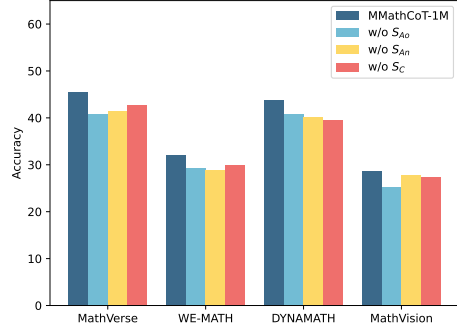


Figure 9: Each synthesis strategy towards different type of source data works well.

¹<https://huggingface.co/Qwen/Qwen2.5-7B-Instruct>

²<https://huggingface.co/Qwen/Qwen2.5-Math-7B-Instruct>

E.2 Selection of External Closed-source MLLM

In this section, we primarily present a comparison of metrics between Gemini-1.5-Flash-002³ and other popular MLLMs, as well as a comparison on partial training data.

Table 11: SFT Performance with 50K data synthesized by two closed-source MLLMs, respectively.

Model	MathVista-GPS	MathVerse	MathVision
URSA-8B w/ GPT-4o	54.1	33.3	18.8
URSA-8B w/ Gemini-1.5-Flash-002	55.1	32.5	18.3

- *Metrics Comparison*: We compare the performance of Gemini-1.5-Flash-002, GPT-4o, and GPT-4o-mini on some math-related tasks, as shown in Table 12. We observe that Gemini-1.5-Flash-002 is a MLLM that performs well on both unimodal and multimodal math tasks, and GPT-4o does not have a significant advantage over it. This, to some extent, ensures the quality of the data synthesis.
- *SFT Performance*: To best illustrate the performance variations, we randomly sampled 50K data sources from MMathCoT-1M, applied three corresponding strategies using GPT-4o, and subsequently conducted SFT. The performance results are shown in Table 11. We observe that using GPT-4o did not provide a clear advantage. However, the construction of MMathCoT-1M and DualMath-1.1M involves approximately 2.7 million API calls. The output token cost of Gemini-1.5-flash-002 is the same as that of GPT-4o-mini and is one-thirty-third of that of GPT-4o⁴. Therefore, Gemini-1.5-Flash-002 becomes a cost-effective choice.

However, we must say that if community researchers can afford the cost of accessing more powerful closed-source models, we expect the results to be even better.

Table 12: Comparison of Model Performance on Math Benchmarks

Model	Avg	MATH	MathVista	MathVerse	MathVision
GPT-4o	55.4	76.6	63.8	50.8	30.4
Gemini-1.5-Flash-002	53.6	79.9	58.4	49.4	26.3
GPT-4o-mini	48.0	70.2	56.7	42.3	22.8

³<https://deepmind.google/technologies/gemini/flash/>

⁴<https://docsbot.ai/models/gemini-1.5-flash-002>

F Implementation Details

F.1 RL Data Curation

After instruction fine-tuning on MMathCoT-1M, the overall accuracy did not exceed 50%. Therefore, we believe it still has the potential to be directly utilized in the RL phase. We collect 20K data with a types mixture ratio similar to that of instruction fine-tuning and conduct a one-time static filtering before RL. Specifically, we use URSA-8B to perform 8 samplings on this 20K data, filtering out examples where all 8 sampling results are either incorrect or correct. This left approximately 15K+ data for training vanilla GRPO and PS-GRPO. We implement PS-GRPO using TRL [100, 102]. The statistics of the RL data can be found in the table 10.

F.2 Parameters and Time Cost

In this section, we provide the specific parameter settings and time costs for the three stages. Our experiments are based on Python 3.10 and PyTorch 2.4.0+cu124. We use AdamW [103] as the optimizer. We use Fully Shared Data Parallel (FSDP) [104] as the distributed training framework. Unless otherwise specified, experiments are conducted on $32 \times$ NVIDIA-H100-HBM3 GPUs by default. Additionally, we provide important parameters used in data construction. During the generation of positive and negative example pairs, we set the *temperature* to 1.0, *n_return_sequences* to 16, and *top_p* to 0.95. In the *BinaryErrorLocating* phase, we set the *temperature* to 0.3, *n_return_sequences* to 16, and *top_p* to 0.95.

We adapt the vLLM [105] framework for the URSA-8B’s architecture (hybrid vision tower + MLP + Qwen2.5-math-Instruct is not originally supported by VLLM) and use it as an acceleration tool during the inference phase. During the data pair generation phase, we use $16 \times$ NVIDIA-H100-HBM3 GPUs for inference, which takes approximately 28 hours. In the *BinaryErrorLocating* phase, we also use $16 \times$ NVIDIA-H100-HBM3 GPUs for inference, taking about 20 hours.

The hyperparameter and time cost used in Stage I and Stage II are demonstrated in Table 13. Since the parameters used in Stage III are somewhat different, we list them separately in Table 14. Recently, much work has provided numerous optimization tricks for GRPO, such as training-time dynamic sampling, clipping higher values, abandoning KL loss, etc [106, 58]. However, to independently verify the effectiveness of PRM-guided reward modeling, we have not added these tricks in either vanilla GRPO or PS-GRPO to ensure a fair and valid verification process. We only do **one-time** difficulty-based data selection before applying RL.

Table 13: Hyperparameter setting and training time cost in Stage I and II.

Hyperparameters & Cost	VL-alignment	Instruction Fine-tuning	PRM Training
Learning Rate	1e-4	1e-5	5e-6
Epoch	1	2	2
Warm-up Ratio	0.02	0.02	0.02
Weight Decay	0.02	0.01	0.02
Batch Size	64	128	128
Trainable Parts	Aligner	Vision Encoder, Aligner, Base LLM	Base LLM
Data Size	860K	1.0M	1.1M
Time Cost	$\sim 3.5h$	$\sim 11h$	$\sim 12h$

F.3 Benchmarks

In this section, we introduce the detailed subtasks and metrics of four used benchmarks to more precisely demonstrate the evaluation.

Figure 10: Statistics of RL data for vanilla GRPO and PS-GRPO.

Statistic	Number
<i>Total Prompts</i>	
- Total number	15.3K
<i>Data Source</i>	
- MathV360K	2.7K
- Multimath-EN	7.5K
- MAVIS-Geo	2.2K
- MAVIS-MetaGen	0.9K
- Geo170K-QA	2.1K
<i>Problem Category Statistics</i>	
- Plane Geometry	4.1K (26.8%)
- Analytic Geometry	1.9K (12.4%)
- Solid Geometry	1.0K (6.5%)
- Algebra	1.1K (7.2%)
- Function	2.9K (19.0%)
- Chart	1.9K (12.4%)
- Textbook QA	0.9K (5.9%)
- Formula	0.8K (5.2%)
- Arithmetic	0.7K (4.6%)

MathVerse MathVerse [72] is a benchmark for testing the reasoning abilities of MLLMs when the information content in text and image modalities varies. Specifically, the models focus on performance in six scenarios: Text-Dominant (TD), Text-Lite (TL), Text-Only (TO), Vision-Intensive (VI), Vision-Dominant (VD) and Vision-Only (VO).

WE-MATH WE-MATH [75] is the first benchmark that decompose composite problems into sub-problems according to the required knowledge concepts. In figure 8, the actual content corresponding to the abbreviations is as follows. Mem: Measurement, PF: Plane Figures, SF: Solid Figures, TMF: Transformations and Motion of Figures, PD: Position and Direction, AL: Angles and Length, UCU: Understanding and Conversion of Units, CPF: Calculation of Plane Figures, UPF: Understanding of Plane Figures, CSF: Calculation of Solid Figures, USF: Understanding of Solid Figures, BTF: Basic Transformations of Figures, CCF: Cutting and Combining of Figures, Dir: Direction, Pos: Position, RoM: Route Map, CCP: Correspondence of Coordinates and Positions.

DYNAMATH DYNAMATH [73] is a benchmark designed to evaluate the robustness of MLLMs in mathematical reasoning. Specifically, it includes tests across multiple dimensions, including Solid Geometry (SG), Plane Geometry (PG), Analytic Geometry (AG), Algebra (AL), Puzzle Test (PT), Graph Theory (GT), Arithmetic (AR), Scientific Figure (SF) and Statistics (ST). It includes 501 seed questions and 5010 generated questions.

GeoQA The GeoQA [40] dataset is a specialized dataset designed for evaluating and training models in the field of geographic question answering. Its test set includes 734 samples.

MathVista MathVista [74] comprises a total of 5 subtasks: Geometry Problem Solving (GPS), Math Word Problem (MWP), Figure Question Answering (FQA), Textbook Question Answering (TQA) and Visual Question Answering (VQA). Like the previous math reasoning works, our model training process does not overly focus on knowledge-intensive tasks (such as VQA and FQA), hence we choose GPS as the primary task.

MathVision MathVision [107] is a large-scale multimodal math reasoning dataset that broadens the disciplinary scope of the multimodal mathematics field. The test set contains 3,040 examples, covering 16 key competencies, and provides reliable testing performance. Specifically, The specific meanings of the various disciplinary indicators in Table 5 are listed as following. Alg: algebra, AnaG: analytic geometry, Ari: arithmetic, CombG: combinatorial geometry, Comb: combinatorics, Cnt: counting, DescG: descriptive geometry, GrphT: graph theory, Log: logic, Angle: metric geometry - angle, Area: metric geometry - area, Len: metric geometry-length, SolG: solid geometry, Stat: statistics, Topo: topology, TransG: transformation geometry.

Evaluation Criteria Our comparison is based on the following criteria: First, we select the results from the official leaderboards of each benchmark. Second, we choose the results from the original papers or technical reports of each model. Finally, we conduct our own inference and evaluation using vLLM [105]. Our evaluation adheres to the rules of the benchmarks themselves, which are as follows:

- **Rule-based Matching:** WEMATH, GeoQA.
- **LLM-as-a-Judge:** MathVista, MathVision, MathVerse, Dynamath.

The prompt for LLM-as-a-Judge is shown in Figure 11.

F.4 Algorithm

In this section, we place the specific process of BIE from Section 3.2 into Algorithm 1. Specifically, the input is a solution that points to an incorrect answer. We set a per-step sampling hyperparameter

Table 14: Hyperparameter setting and training time cost in Stage III.

Hyperparameters / Cost	Value
Epochs	2
Learning Rate	2e-6
Temperature	1.0
Rollout number per prompt	8
Prompt Max Length	6048
Output Max Length	3072
Precision	bf16
Train Batch Size	512
KL Coefficient	0.003
Data size	15K
Time Cost	~18h

LLM-as-a-Judge

Below are two answers to a math question. Question is [Question], [Standard Answer] is the standard answer to the question, and [Model_answer] is the answer extracted from a model's output to this question.

Determine whether these two answers are consistent.

Please note that only when the [Model_answer] completely matches the [Standard Answer] means they are consistent. For non-multiple-choice questions, if the meaning is expressed in the same way, it is also considered consistent, for example, 0.5m and 50cm.

If they are consistent, Judement is 1; if they are different, Judement is 0.

Example 1:

[Question]: Write the set of numbers represented on the number line in interval notation.

[Standard Answer]: (-2,1]

[Model_answer] : Extracted Answer: \((-2, 1)\)

Judgement: 0

Example 2:

[Question]: As shown in the figure, circle O has a radius 1.0, if angle BAC = 60.0, then the length of BC is ()

Choices:

A:2

B: $2\sqrt{3}$

C: $\sqrt{3}$

D: $2\sqrt{2}$

[Standard Answer]: C

[Model_answer] : B: $2\sqrt{3}$

Judgement: 0

Example 3:

[Question]: Find the domain and range of the function f using interval notation.

[Standard Answer]: domain: [-4, 0) and range: (-3, 1]

[Model_answer] : Range: \((-4, 1]\)

Judgement: 0

Example 4:

[Question]: As shown in the figure, circle O has a radius 1.0, if angle BAC = 60.0, then the length of BC is ()

Choices:

A:2

B: $2\sqrt{3}$

C: $\sqrt{3}$

D: $2\sqrt{2}$

[Standard Answer]: C

[Model_answer] : null

Judgement: 0

OK. Now let's begin:

[Question]: {QuestionText}

[Standard Answer]: {AnswerText}

[Model answer]: {ResponseText}

Your response:

Figure 11: LLM-as-a-Judge prompt used for answer matching.

N_{mid} . Initially, we set the start and end points of the search range to Step 1 and Step N , respectively. We first consider the mc value of Step $(1+N)//2$. If it is positive, it indicates that the first totally erroneous step occurs in the latter half; otherwise, we look in the first half. This reduces the number of searches to $\mathcal{O}(\log N)$.

Besides, we introduce the process of PS-GRPO in Algorithm 2. This process involves merging of outcome reward and process-as-outcome reward, and subsequent relative advantages calculation.

Algorithm 1 BinaryErrorLocating

```
1: Input: Solution set  $S = \{y_i | i = 1, 2, \dots, N\}$ , mid step sampling num  $N_{mid}$ .
2: for  $i = 1$  to  $N$  do
3:    $l \leftarrow 0, r \leftarrow \text{StepLen}(y_i)$                                  $\triangleright$  Define start and end index.
4:   while  $l < r$  do
5:      $mid \leftarrow \lfloor (l + r)/2 \rfloor$ 
6:      $\text{MID\_RES} \leftarrow \mathcal{F}(\{y_{i,1}, y_{i,2}, \dots, y_{i,mid}\}, N_{mid})$        $\triangleright$  Sampling from mid step.
7:     if VERIFY(MID_RES) does not contain True then       $\triangleright$  Judge sampling's final answer.
8:        $r \leftarrow mid$ 
9:     else
10:       $l \leftarrow mid + 1$ 
11:    end if
12:  end while
13:   $e_i \leftarrow \text{WRONGSTEPLABELING}(y_i, l)$                                  $\triangleright$  Collect sequential labels of  $y_i$ .
14:  ErrorLocatingSet.append{ $e_i$ }
15: end for
16: Output: ErrorLocatingSet
```

Algorithm 2 PS-GRPO

```
1: Input: Policy model  $\pi_\theta$ , Process Reward Model  $\phi_\theta$ , train dataset  $D_{RL} = \{I_i, Q_i, Y_i\}_{i=1}^N$ .
2: ErrorLocatingSet  $\leftarrow []$ 
3: for Epoch = 1 to  $N$  do
4:   for Batched data  $\{I, Q, Y\}$  in  $D_{RL}$  do
5:     Generate rollouts of  $\{I, Q\}$ :  $\{c^j\}_{j=1}^M \sim \pi_\theta$ 
6:     Calculate process reward sets  $S = \{(p_1, p_2, \dots, p_{|c_j|}) \sim \phi_\theta(c^j) | 0 < j < M\}$ 
7:     Calculate reward  $\{r^j\}_{i=1}^M$  by Equation 5 and 6.
8:     Calculate relative advantages  $\{\hat{A}^j\}_{i=1}^M$  using Equation 7.
9:     Update policy model  $\pi_\theta$  using Equation 8.
10:   end for
11: end for
12: Output: Updated policy model  $\pi_\theta$ .
```

G Prompt Design

G.1 Prompt Utilized in MMathCoT-1M Synthesis

In this section, we provide the specific prompts for three-module data synthesis. Additionally, Gemini-1.5-Flash is a model that is very sensitive to prompts and parameters in practical experience, and we will share detailed adjustment experiences.

CoT Expansion CoT expansion prompt for answer-only data source can be seen in Figure 12. We order the Gemini-1.5-flash to give a reasonable process directing to the ground-truth. After the execution, we find that the outputs is not so clear. The model sometimes will give trajectories that include “we must trust the answer” or “let me assume”. We identify these phrases as signals that the model can not solve the problem naturally and independently. We will filter these samples.

Analysis Rewriting Rewriting prompt for analysis-formatted data synthesis is illustrated in Figure 13. For solutions in an analytical format, we transform them into clear step-by-step format trajectories. During this process, Gemini-1.5-flash-002 does not exhibit significant questioning or make conditional requests. We improve data quality through reorganization and polishing of the language logic.

Format Unified By employing a unified format prompt shown in Figure 14 to modify the reasoning styles of plan-and-reasoning and symbolic approaches, we are able to extract a more natural language process aligned with the pre-training style. A single example is sufficient to elicit perceptually favorable responses.

CoT Distillation

For a question, you need to provide a **step-by-step solution** that directs to the given right answer. You must **trust** the given correct answer and avoid **making any requests** for additional information and **any suspect**.

Example 1:

Question: Given that points A, B, and C lie on circle O and angle AOB measures 80.0 degrees, what is the measure of angle ACB? Choices:

- A: 80°
- B: 70°
- C: 60°
- D: 40°

Provided answer: D

Your Response:

Step 1: Identify the given information: angle AOB = 80°.

Step 2: Apply the relevant theorem: angle ACB = 1/2 angle AOB (inscribed angle theorem).

Step 3: Substitute the given value: angle ACB = 1/2 * 80° = 40°.

Step 4: State the answer: The answer is D.

†Answer: D

Example 2:

Question: As shown in the diagram, AB is the diameter of circle O. EF and EB are chords of circle O.

Connecting OF, if angle AOF = 40°, then the degree of angle E is (). Choices:

- A: 40°
- B: 50°
- C: 55°
- D: 70°

Provided answer: D

Your Response:

Step 1: Given angle AOF = 40°.

Step 2: Angles AOF and FOB are supplementary, meaning they add up to 180°. Therefore, angle FOB = 180° - 40° = 140°.

Step 3: Angle E is half of angle FOB. Therefore, angle E = 0.5 * 140° = 70°.

Step 4: The answer is D.

†Answer: D

Now, let's begin.

Question: {QuestionText}

Provided answer: {SolutionText}

Your Response:

Figure 12: CoT expansion prompt for answer-only data.

Double-checking After completing the above three points, we apply an LLM-as-a-judge for double-checking the synthesized data, ensuring that the solutions do not contain unreasonable processes, such as untimely questioning, conditional requests, or reasoning loops. The specific prompt design is shown in Figure 15. After this layer of filtering, we obtain the final MMathCoT-1M.

G.2 Prompt Utilized in DualMath-1.1M Synthesis

In this section, we demonstrate the prompts used in MIE.

- **Geometry Problem:** For geometry problem, we prompt the Gemini-1.5-Flash-002 to first identify key geometry features in the figure. We then order it to introduce a misinterpretation on these elements. Finally, use the wrong information to execute a misleading solution. The total design can be seen in Figure 16.

Analysis Rewriting

I have a mathematical problem-solving process here, and both the process and the final answer are completely correct. I hope you can solve it in a **different way** based on the existing solution process, ensuring that the process and results are correct, especially the reasoning results **remain consistent with the original**.

Please remember the following instructions:

1. You must **trust** that the solution and final answer is correct, and you **do not need to review or refute it**.
2. Your transcription must be **semantically coherent**.
3. You **cannot make requests** like “require more information” or similar, because the given conditions are sufficient and the solution is definitely correct.
4. You can rewrite from multiple perspectives, such as **providing different solutions** to the problem or adopting **different textual styles**.
5. You must end with ‘†Answer:’, filling in the definitive answer provided.

Question:

{QuestionText}

Correct Solution:

{SolutionText}

Give the rewritten solution in the following format:

Step 1: ...

Step 2: ...

...

†Answer: ...

Your solution:

Figure 13: Analysis rewriting prompt for analysis-formatted data.

- **Charts & Function:** For ChartQA and math functions, we prompt Gemini-1.5-Flash-002 to first check the fine-grained data points. We then attempt to insert spatially similar data to induce a misinterpretation. This subsequently leads to incorrect solutions for automatic labeling.
- **LLM-as-a-Judge:** For chart reasoning and function problem, we execute similar process on Gemini-1.5-Flash-002. We place it in Figure 17.

H Case Study

H.1 Showcase on Best-of-N Evaluation

To more clearly illustrate the effectiveness of URSA-8B-RM in BoN evaluation, a case on MathVista-GPS is demonstrated (Figure 18). This case shows that URSA-8B-RM is sensitive to false theorem application and misunderstandings of angle-number relations. The good property not only enables URSA-8B-RM to perform well in BoN evaluation but also endows it with the potential to identify more valuable learning samples in online reinforcement learning.

H.2 Process of Misinterpretation Insertion Engine

As shown in Figure 19, MIE performs three main actions: First, it interprets the mathematical information in the image. Then, it replaces key information at a selected step. Finally, it continues reasoning based on the modified conditions.

H.3 Failure Pattern in Process During GRPO

In this section, we intuitively reveal through examples why PS-GRPO works effectively. We first introduce the concept of false-positive rollouts, which are rollouts that, despite reaching the correct answer, do not provide perfect intermediate actions to arrive at the solution. They can generally be

Format Unified

You are given a question and a solution, and your task is to translate the reasoning process from mathematical language into a style of natural language reasoning.

Instructions:

- Convert the formal mathematical solution into a **natural language explanation**.
- Use "Step X:" to separate each step.
- End the solution with "†Answer: [final answer]".
- Ensure the explanation is clear, concise, and free of formal mathematical symbols unless absolutely necessary.
- ****You must strictly follow the provided solution steps and final answer. Do not modify, correct, or reinterpret any part of the solution.****

Example:

Question:

Given that OB is perpendicular to OA, line CD passes through point O, and $\angle AOC = 20^\circ$, then $\angle BOD = ?$

Formal Solution:

Step 1 (Definition of Perpendicular): $\because OB \perp OA, \therefore \angle BOA = 90^\circ$.

Step 2 (Given condition): $\because \angle AOC = 20^\circ, \therefore \angle BOC = 90^\circ - \angle AOC = 90^\circ - 20^\circ = 70^\circ$.

Step 3 (Supplementary angles property): $\angle BOD = 180^\circ - \angle BOC = 180^\circ - 70^\circ = 110^\circ$.

Answer: \boxed{110}

Your Response:

Step 1: Since OB is perpendicular to OA, we have that angle BOA is 90 degrees.

Step 2: Given that angle AOC is 20 degrees, it follows that angle BOC is 90 degrees minus angle AOC, which is 70 degrees.

Step 3: Using the property of supplementary angles, angle BOD is 180 degrees minus angle BOC, which is 110 degrees.

†Answer: 110

Now, let's begin!

Question:

{QuestionText}

Solution:

{SolutionText}

** Your Response:

Figure 14: Format unify prompt for mathematical and symbolic reasoning style data.

divided into two categories: (i) the lack of visual condition alignment. Solutions in this category exhibit inconsistencies in reasoning regarding basic visual factors such as edge relationships, coordinate values, and theorem applications, revealing deficiencies in the pretraining phase, as shown in Figure 20. (ii) the exploitation of shortcut patterns. These rollouts do not go through key steps but are guided directly to the correct answer after basic descriptions due to the high correlation between image features and problem-solving patterns during pretraining or SFT, as shown in Figure 21. Therefore, PS-GRPO suppresses the advantageous direction brought by these erroneous actions through the sensitivity of the PRM in online RL for error identification. This leads to a more optimal paradigm that combines outcome rewards with process reward-based penalties.

H.4 Cases on How Naive Process Reward Modeling Fails

In this section, we elaborate on the two fundamental flaws of process reward guided RL mentioned in Section 4 and present some cases for illustration. In online RL, models can easily recognize the patterns for obtaining process rewards, leading to conservative analyses and concise responses as they sidestep PRM scrutiny. As shown in Figure 22, we have observed that the model often follows a distinct reasoning pattern. They initially read and analyze the given conditions comprehensively, but then make incorrect decisions based on this analysis, leading to wrong answers. This indicates that

Double Checking

You are tasked with evaluating whether a provided solution **aligns precisely** with a given standard answer. Your evaluation must strictly adhere to the following criteria:

Solution Fidelity

- ****Certainty****: The solution must be free of any elements of doubt or speculative reasoning. Avoid using phrases that imply uncertainty or hypothetical reasoning, such as “more conditions are needed”, “the answer seems questionable”, “let us assume”, “the provided solution seems wrong” or any similar expressions. The solution should be presented with confidence and clarity, reflecting a definitive and well-supported conclusion.

Solution Consistency

- ****Alignment with Standard Answer****: The final conclusion of the solution must match the given standard answer exactly. The reasoning process should directly and unequivocally lead to the provided answer without deviation. Ensure that there are no discrepancies between the solution's conclusion and the standard answer.

Evaluation Process

1. ****Analyze the Solution****: Carefully review the logical steps and reasoning used in the solution to ensure they are sound and lead directly to the conclusion.

2. ****Compare with Standard Answer****: Verify that the conclusion of the solution is **identical to the standard answer** provided.

3. ****Provide Judgment****: Based on your analysis, offer a clear and concise judgment finally:

- Respond with “**Judgment: yes**” if the solution’s conclusion is consistent with the given standard answer.

- Respond with “**Judgment: no**” if the solution’s conclusion does not match the standard answer.

Example Structure

- ****Question****:

{QuestionText}

- ****Standard Answer****:

{AnswerText}

- ****Solution Answer****:

{SolutionText}

Your Response

Figure 15: Double-checking prompt for ensuring high-quality and appropriate trajectories in synthesized CoT reasoning data.

when explicitly modeling process rewards, models can easily focus on processes that seem "correct" in isolation. However, these processes may not be genuinely helpful for the final outcome and instead may lead the model to prioritize high process rewards over accuracy.

Misinterpretation Insertion for Geometry Problem

You are given a geometry problem with an image and its solution. Your task is to introduce errors into the solution by misreading the diagram and generate an incorrect answer.

Instructions:

- Your response involves three Stages:

** Stage 1: Analyze the Correct Solution **: Identify where in the solution diagram information is extracted. Note these areas as **potential points for introducing misinterpretations**.

** Stage 2: Introduce a Misinterpretation **: Choose one of the identified points from Stage 1 and **alter it to create a misleading scenario**. Integrate this misinterpretation naturally into the solution.

** Stage 3: Continue Reasoning **: Based on the misinterpretation from Stage 2, **continue the reasoning** process to derive an incorrect final answer.

- Ensure the misreading is **naturally integrated** without explicit statements about making a misinterpretation. When describing corrupted solution, avoid showing the misleading thought process. You must respond in a typical problem-solving style.

- Remember that the `<pos>` and `<neg>` tags only need to appear at the end of each Step X. Do not repeat them between Step X and Step X+1, even if the reasoning process for that step spans many lines.

- Remember that once a step is marked as `<neg>`, all subsequent steps are also considered `<neg>`.

- 'Answer' is the final answer, and it should not be tagged.

- You **cannot** tag an unaltered step with `<neg>` without misinterpreting it. You must misinterpret the step if you are tagging it with `<neg>`.

- Words that imply misinterpretation, such as '**misread**' '**incorrect**' or '**incorrectly assume**' must not appear in your response under any circumstances.

- The misinterpretation action in Stage 3 should be **consistent** with what was planned in Stage 2.

Question:

{QuestionText}

Solution:

{SolutionText}

** Your response:

Figure 16: Misinterpretation insertion for geometry-related problems.

Misinterpretation Insertion for Charts & Function

You are given a math problem with a **coordinate axis or chart** and its solution. Your task is to introduce errors into the solution by misreading the image or chart and generate an incorrect solution.

Instructions:

- Your response involves three Stages:

** Stage 1: Image Information Extraction **: Identify where in the solution diagram information is extracted.

Note these areas as potential points for introducing misinterpretations.

** Stage 2: Introduce a Misinterpretation **: Choose one of the identified points from Stage 1 and alter it to create a misreading scenario. Integrate this misinterpretation naturally into the solution.

** Stage 3: Continue Reasoning **: Based on the misinterpretation from Stage 2, continue the reasoning process to derive an incorrect final answer.

- Ensure the misreading is naturally integrated without explicit statements about making a misinterpretation.

When describing corrupted solution, avoid showing the misleading thought process. You must respond in a typical problem-solving style.

- Remember that the `<pos>` and `<neg>` tags only need to appear at the end of each Step X. Do not repeat them between Step X and Step X+1, even if the reasoning process for that step spans many lines. Remember that once a step is marked as `<neg>`, all subsequent steps are also considered `<neg>`.

- '†Answer:' is the final answer, and it should not be tagged.

- You cannot tag an unaltered step with `<neg>` without misinterpreting it. You must misinterpret the step if you are tagging it with `<neg>`.

- Words that imply misinterpretation, such as 'misread' 'incorrect' or 'incorrectly assume' must not appear in your response under any circumstances.

- The misinterpretation action in Stage 3 should be consistent with what was planned in Stage 2.

Question:

{QuestionText}

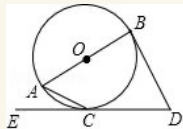
Solution:

{SolutionText}

** Your response:

Figure 17: Misinterpretation insertion for function and chart-related problems.

URSA-RM-8B as Verifier



Problem:

As shown in the figure, AB is the diameter of circle O, DB and DC are respectively tangent to circle O at points B and C. If $\angle ACE = 25.0^\circ$, then the degree of $\angle D$ is ()
 A. 50° B. 55° C. 60° D. 65°

Solution 1:

Step 1: We are given that AB is the diameter of circle O, and DB and DC are tangents to circle O at points B and C respectively. We are also given that $\angle ACE = 25^\circ$. **0.93**

Step 2: Since DB and DC are tangents to circle O from the same point D, we know that $DB = DC$. This means that triangle DBC is an isosceles triangle. **0.95**

Step 3: In triangle DBC, let $\angle DBC = \angle DCB = x$. Since the sum of angles in a triangle is 180° , we have $\angle BDC + \angle DBC + \angle DCB = 180^\circ$. Therefore, $\angle BDC + 2x = 180^\circ$. **0.91**

Step 4: Since AB is the diameter, $\angle ACB$ is a right angle (90°). In right-angled triangle ACB, we have $\angle CAB + \angle ABC = 90^\circ$. **0.93**

Step 5: We are given that $\angle ACE = 25^\circ$. Since $\angle ACB = 90^\circ$, we have $\angle ECB = 90^\circ - 25^\circ = 65^\circ$. **0.98**

Step 6: In triangle DBC, $\angle DBC + \angle DCB + \angle BDC = 180^\circ$. Since DB and DC are tangents, $\angle DBC = \angle DCB = 90^\circ - 25^\circ = 65^\circ$. Therefore, $65^\circ + 65^\circ + \angle BDC = 180^\circ$, which gives $\angle BDC = 180^\circ - 130^\circ = 50^\circ$. **0.98**

Step 7: Therefore, $\angle D = \angle BDC = 50^\circ$. **0.88**

†Answer: A

Solution 2:

Step 1: Identify the relevant angles. We are given that $\angle ACE = 25^\circ$. We want to find $\angle D$. **0.99**

Step 2: Recognize the relationship between the angles. Since AB is the diameter of circle O, and DB is tangent to circle O at B, we know that $\angle ABD$ is a right angle (90°). Also, since DB and DC are tangents from the same point D to circle O, we know that $DB = DC$. This means that triangle DBC is an isosceles triangle. **0.94**

Step 3: Use the property of isosceles triangles. In isosceles triangle DBC, $\angle DBC = \angle DCB$. Let's denote this angle as x . The sum of angles in triangle DBC is 180° . Therefore, $\angle BDC + \angle DBC + \angle DCB = 180^\circ$. Substituting the values, we get $\angle BDC + x + x = 180^\circ$, which simplifies to $\angle BDC + 2x = 180^\circ$. **0.90**

Step 4: Relate the angles. $\angle ACE$ is an inscribed angle subtending the arc BC. **The angle subtended by the same arc at the center is twice the inscribed angle. Therefore, $\angle BOC = 2 * \angle ACE = 2 * 25^\circ = 50^\circ$** . **0.46**

Step 5: Find the angle $\angle BDC$. Since $\angle ABD$ is a right angle (90°), and $\angle BOC = 50^\circ$, we can find $\angle BDC$. In quadrilateral ABCD, the sum of angles is 360° . We have $\angle DAB + \angle ABC + \angle BCD + \angle CDA = 360^\circ$. Since $\angle ABC = 90^\circ$ and $\angle BCD = x$, we have $\angle DAB + 90^\circ + x + \angle CDA = 360^\circ$. **0.67**

Step 6: Solve for x . We know that $\angle BDC + 2x = 180^\circ$. Also, **$\angle BDC + \angle DAB = 180^\circ$ (angles on a straight line)**.

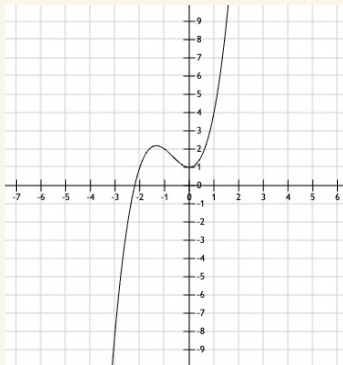
Therefore, $\angle DAB = 180^\circ - \angle BDC$. Substituting this into the equation from step 5, we get $(180^\circ - \angle BDC) + 90^\circ + x + \angle CDA = 360^\circ$. This simplifies to $270^\circ - \angle BDC + x + \angle CDA = 360^\circ$. **0.65**

Step 7: Determine $\angle D$. Since triangle DBC is isosceles, $\angle DBC = \angle DCB = x$. Also, $\angle BDC + 2x = 180^\circ$. We know that $\angle ACE = 25^\circ$, which is an inscribed angle subtending arc BC. The central angle subtending the same arc is $2 * 25^\circ = 50^\circ$. This central angle is $\angle BOC$. In triangle OBC, OB = OC (radii), so it's an isosceles triangle. Therefore, $\angle OBC = \angle OCB = (180^\circ - 50^\circ)/2 = 65^\circ$. **Since $\angle OBC$ and $\angle DBC$ are supplementary, $\angle DBC = 180^\circ - 65^\circ = 115^\circ$** . However, this is incorrect. Let's reconsider. Since $\angle ACE = 25^\circ$, the arc BC subtends an angle of 50° at the center. In triangle OBC, OB = OC, so $\angle OBC = \angle OCB = (180^\circ - 50^\circ)/2 = 65^\circ$. Therefore, $\angle D = 65^\circ$. **0.47**

†Answer: D

Figure 18: Case of URSA-8B-RM serving as a verifier in Best-of-N evaluation.

Showcase of how MIE works



Problem:

Given a cubic function $y = ax^3 + bx^2 + cx + d$, please determine the values of a, b, c and d.

Original Solution:

Step 1: I first need to identify the points that the graph passes through, and then substitute these points into the equation to solve for the values of a, b, c, and d.

Step 2: I find some points below: P1: (-3, -8) P2: (0, 1) P3: (-2, 1) P4: (-1, 2)

...

Step N: a=1, b=2, c=0, d=1

Gemini's response:

Information Extraction: I see this question is highly related to the coordinates of points on the line. The line appears in the third quadrant, second quadrant, and first quadrant.

Misinterpretation Insertion: A simple method is to introduce incorrect point coordinates to reach a wrong conclusion. As the correct solution states, the coordinates of point P1 are (-3, -8), but we easily replace them with (-3, -7) as a premise.

Continue Reasoning:

Step 1: I first need to identify the points that the graph passes through, and then substitute these points into the equation to solve for the values of a, b, c, and d. <pos>

Step 2: I find some points below: P1: (-3, -7) P2: (0, 1) P3: (-2, 1) P4: (-1, 2). <neg>

Step 3: Using P1: (-3, -7),

$$-7 = a(-3)^3 + b(-3)^2 + c(-3) + 1$$

$$-7 = -27a + 9b - 3c + 1$$

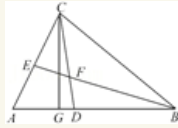
$$-8 = -27a + 9b - 3c \quad <\text{neg}>$$

...

$$\text{Step N: } a = \frac{5}{6}, b = \frac{3}{2}, c = -\frac{1}{3}, d = 1. \quad <\text{neg}>$$

Figure 19: Case from MIE. We introduce specific step-level perception errors and continue false reasoning to construct a correctnesses-labeled solution.

Rollouts Analysis on Process (I)



Problem:

In the diagram, point F is the intersection of the angle bisectors CD and BE of triangle ABC, and CG is perpendicular to AB at point G. If angle ACG is 32 degrees, what is the measure of angle BFC?

Perfect Rollout:

Step 1: Recognize that CD and BE are angle bisectors, so point F is the incenter of triangle ABC.

Step 2: Since CG is perpendicular to AB, triangle CGA is a right triangle.

Step 3: In triangle CGA, using the fact that the sum of angles is 180°, calculate angle CAG: $\text{angle CAG} = 90^\circ - \text{angle ACG} = 90^\circ - 32^\circ = 58^\circ$.

Step 4: Since CD is the angle bisector of angle ACB, $\text{angle ACD} = \text{angle BCD} = 1/2 \text{ angle ACB}$.

Step 5: Let angle ACB = 2φ . Then angle ACD = angle BCD = φ .

Step 6: Similarly, BE is the angle bisector of angle ABC, so angle ABE = angle EBC = $1/2 \text{ angle ABC}$.

Step 7: Let angle ABC = 2θ . Then angle ABE = angle EBC = θ .

Step 8: In triangle ABC, the sum of angles is 180°. So, $\text{angle BAC} + \text{angle ABC} + \text{angle ACB} = 180^\circ$. Substituting $\text{angle BAC} = 58^\circ$, and $\text{angle ABC} = 2\theta$, $\text{angle ACB} = 2\varphi$. So, $58^\circ + 2\theta + 2\varphi = 180^\circ$, which simplifies to $\varphi + \theta = 61^\circ$.

Step 9: In triangle BFC, the sum of angles is 180°. So, $\text{angle BFC} + \text{angle FBC} + \text{angle FCB} = 180^\circ$.

Step 10: Substitute angle FBC = φ and angle FCB = θ . So, $\text{angle BFC} + \varphi + \theta = 180^\circ$. From step 8, $\varphi + \theta = 61^\circ$, so $\text{angle BFC} = 180^\circ - 61^\circ = 119^\circ$.

†Answer: 119 °

False-positive Rollout:

Step 1: Recognize that CD and BE are angle bisectors, so point F is the incenter of triangle ABC.

Step 2: Since CG is perpendicular to AB, triangle CGA is a right triangle.

Step 3: In triangle CGA, using the fact that the sum of angles is 180°, calculate angle CAG: $\text{angle CAG} = 90^\circ - \text{angle ACG} = 90^\circ - 32^\circ = 58^\circ$.

Step 4: $\text{Angle BFC} = 180^\circ - \text{angle CDE}$. CD is the angle bisector of angle ACB, $\text{angle ACD} = \text{angle BCD} = 1/2 \text{ angle ACB}$.

Step 5: We have $\text{angle CDE} = \text{angle ACD} = \text{angle BCD} = 1/2 \text{ angle ACB}$.

Step 6: Since $\text{angle ACB} + \text{angle ACG} = 180^\circ$, $\text{angle ACB} = 180^\circ - 58^\circ = 122^\circ$.

Step 7: Substitute $\text{angle ACB} = 122^\circ$, $\text{angle ACD} = 1/2 * 122^\circ = 61^\circ$.

Step 8: Substitute $\text{angle ACD} = 66^\circ$, $\text{angle BFC} = 180^\circ - 61^\circ = 119^\circ$.

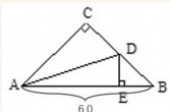
†Answer: 119 °

Analysis:

In this example, false-positive rollout leads to numerous instances of [image-text perception inconsistency](#), and such behavior should not be encouraged in reasoning, even if it happens to yield the correct result.

Figure 20: False positive rollout analysis I.

Rollouts Analysis on Process (II)



Problem:

As shown in the figure, $AC = BC$, AD bisects angle CAB , then the perimeter of triangle DBE is () Choices: A:6cm B:7cm C:8cm D:9cm

Perfect Rollout:

Step 1: The angle bisector states that a point on an angle bisector is equidistant from the two sides of the angle. Since AD bisects angle CAB , $DC \perp AC$, $DE \perp AB$, we conclude that $DC = DE$.

Step 2: Since angle $C =$ angle $AED = 90^\circ$, angle $CAD =$ angle EAD , we have triangle $ACD \cong$ triangle AED .

Step 3: We substitute AC with BC , so $BC = AE$.

Step 4: The perimeter of triangle DBE equals to $DB + BE + DE$, notice that $AE + BE = AB$

Step 5: From the diagram. $AB = 6\text{cm}$

Step 6: The answer is 6cm.

†Answer: A 

False-positive Rollout:

Step 1: Look at the figure and notice that $AC = BC$, so triangle ABC must be isosceles.

Step 2: AD is the angle bisector of angle CAB . Hmm, so it splits angle A into two equal parts.

Step 3: DE is perpendicular to AB .

Step 4: The question asks for the perimeter of triangle DBE . I need to find the lengths of DB , BE , and DE .

Step 5: Since ABC is isosceles with $AC = BC$, angles at A and B are equal.

Step 6: Maybe triangle DBE is related to triangle ABC in some way.

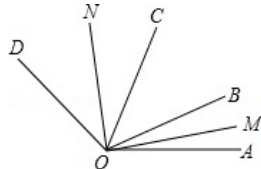
Step 7: Let me guess that the perimeter of DBE is equal to AB . If AB is 6 cm, then the perimeter of DBE would be 6 cm. So the answer is A.

†Answer: A 

Analysis:

This type of learning pattern makes problems very difficult to solve when shortcuts in numerical and geometric relationships point in the wrong direction.

Figure 21: False positive rollout analysis II.



Question:

As shown in the figure: $\angle AOB : \angle BOC : \angle COD = 2 : 3 : 4$, ray OM and ON bisect $\angle AOB$ and $\angle COD$ respectively, and $\angle MON = 84^\circ$, then $\angle AOB$ is ().

Solution:

Step 1: Look at the diagram and note the angles $\angle AOB$, $\angle BOC$, and $\angle COD$ are in the ratio 2:3:4.

Step 2: Recognize OM and ON bisect $\angle AOB$ and $\angle COD$, creating smaller angles.

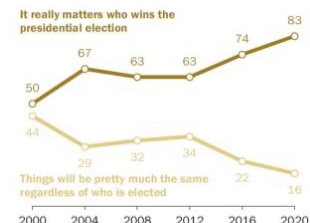
Step 3: Use the given $\angle MON = 84^\circ$ to set up an equation based on the ratios and angle bisectors.

Step 4: Solve the equation $\angle AOB = 2 / (2 + 3 + 4) * 84^\circ = 18.66^\circ$.

†Answer: $\angle AOB$ is 18.66° .

In 2000, just half of voters said it 'really mattered' who won the presidency; this year, 83% express this view

% of registered voters who say ...



Notes: Based on registered voters. Volunteered and don't know responses not shown. Data for prior years from June surveys. Source: Telephone survey of U.S. adults conducted July 23-Aug. 4, 2020.

PEW RESEARCH CENTER

Question:

As shown in the figure: $\angle AOB : \angle BOC : \angle COD = 2 : 3 : 4$, ray OM and ON bisect $\angle AOB$ and $\angle COD$ respectively, and $\angle MON = 84^\circ$, then $\angle AOB$ is ().

Solution:

Step 1: The dark brown line represents voters who think it really matters, showing an increasing trend from 50% in 2000 to 83% in 2020. The light brown line represents voters who think things will be much the same, showing a decreasing trend from 44% in 2000 to 16% in 2020.

Step 2: We need to know the least value of the light brown graph to the leftmost value of the dark brown graph.

Step 3: The ratio of the least value of the light brown graph and the leftmost value of the dark brown graph is 16:67.

†Answer: 16:67.

Figure 22: Bad case analysis on two process reward modeling variants.